Research Square

Preprints are preliminary reports that have not undergone peer review.
They should not be considered conclusive, used to inform clinical practice,
or referenced by the media as validated information.

Activity–selectivity engineering of waste-derived CaO catalysts via KOH and ZnO surface modification for coconut biodiesel production

Victoria Soares
Universidade Federal do Rio Grande do Norte
Joao Sousa
Universidade Federal do Rio Grande do Norte
Luciene Santos
Universidade Federal do Rio Grande do Norte
Marcio Bezerra
mbdbezerra@uesc.br

Universidade Estadual de Santa Cruz

Research Article

Keywords: Biodiesel, Coconut oil, Eggshell waste, Heterogeneous catalyst, Waste valorization

Posted Date: November 12th, 2026

DOI: https://doi.org/10.21203/rs.3.rs-11443424/v1

License: This work is licensed under a Creative Commons Attribution 4.0 International License.
Read Full License

Additional Declarations: No competing interests reported.

Activity–selectivity engineering of waste-derived CaO catalysts via KOH and ZnO surface modification for coconut biodiesel production

Victoria Victor Soares
Universidade Federal do Rio Grande do Norte (UFRN), Natal, Brazil
soaresvictoria870@gmail.com

João Fernandes de Sousa
Universidade Federal do Rio Grande do Norte (UFRN), Natal, Brazil
joao.sousa@ufrn.br

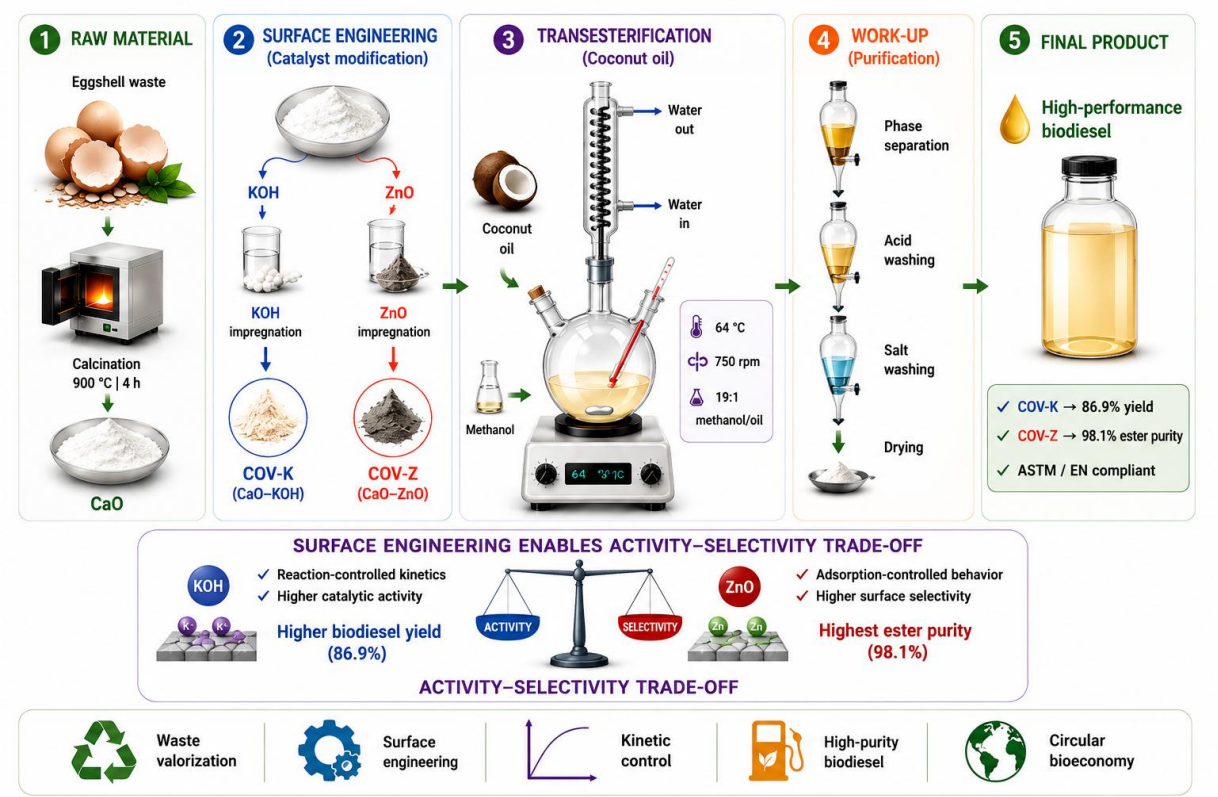
Luciene da Silva Santos
Universidade Federal do Rio Grande do Norte (UFRN), Natal, Brazil
gisl.oliveira@outlook.com

Marcio Barbalho Dantas Bezerra*
Universidade Estadual de Santa Cruz (UESC), Ilhéus, Brazil
***Corresponding author**: mbdbezerra@uesc.br

Highlights

- Waste-derived CaO catalysts were engineered to control activity and selectivity.
- KOH incorporation promoted reaction-controlled catalytic behaviour.
- ZnO incorporation favoured adsorption-controlled selective transesterification.
- A clear activity–selectivity trade-off was experimentally demonstrated.
- Surface engineering established a design framework for circular biofuels.

Graphical Abstract



Abstract

The development of sustainable heterogeneous catalysts for biodiesel production requires not only high conversion efficiency, but also precise control over catalytic activity and product selectivity. However, the influence of surface modification on the activity–selectivity balance of waste-derived CaO catalysts remains poorly understood. In this study, eggshell-derived CaO catalysts were chemically modified with KOH and ZnO in order to investigate how surface

engineering affects catalytic behaviour during coconut oil transesterification. The catalysts were structurally and compositionally characterised by X-ray diffraction (XRD), Fourier transform infrared spectroscopy (FTIR), scanning electron microscopy (SEM), X-ray fluorescence (XRF), energy-dispersive spectroscopy (EDS), and thermogravimetric analysis (TG/DTG), confirming the successful conversion of $CaCO_3$ into catalytically active CaO, incorporation of potassium- and zinc-containing phases, and significant changes in surface morphology and thermal stability after modification. Under fixed reaction conditions (methanol-to-oil molar ratio of 19:1, 1.5 wt% catalyst, 64 °C, 120 min), a clear activity–selectivity trade-off was identified. The KOH-modified catalyst exhibited the highest biodiesel yield (86.9%) and the highest pseudo-first-order kinetic constant (0.0223 min^{-1}), suggesting enhanced catalytic activity and predominantly reaction-controlled behaviour. In contrast, the ZnO-modified catalyst achieved the highest methyl ester content (98.1%) and showed better agreement with pseudo-second-order kinetics, suggesting a greater contribution of adsorption-mediated surface interactions. Biodiesel characterisation by GC-FID, FTIR, TG/DTG, viscosity, and density analyses confirmed the formation of high-quality fatty acid methyl esters compliant with fuel quality standards. Taken together, these findings indicate that chemical modification of waste-derived CaO catalysts enables the rational tuning of catalytic activity and ester selectivity, providing mechanistic insights for the rational design of waste-derived heterogeneous catalysts for sustainable biofuel production within circular economy systems.

Keywords: Biodiesel; Coconut oil; Eggshell waste; Heterogeneous catalyst; Waste valorization.

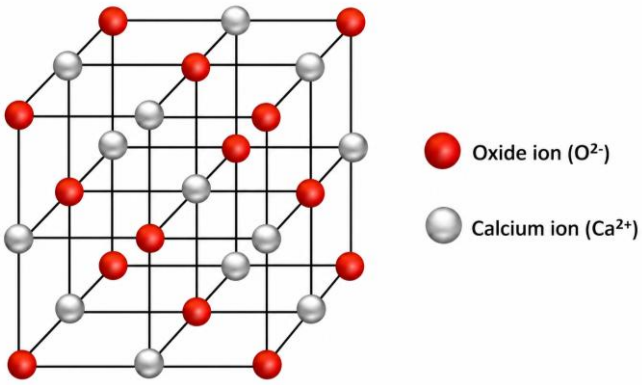
1. Introduction

The global transition towards low-carbon energy systems has intensified the search for renewable fuels capable of reducing greenhouse gas emissions while maintaining compatibility with existing energy infrastructure [1,2,3]. Among the available alternatives, biodiesel has emerged as a particularly attractive option due to its biodegradability, low toxicity, renewable origin, and direct applicability in compression ignition engines [4,5,6,7]. Nevertheless, the large-scale implementation of biodiesel production remains strongly dependent on the development of economically viable and environmentally sustainable catalytic systems [8,9,10].

Transesterification is the most widely adopted route for biodiesel synthesis, involving the conversion of triglycerides into fatty acid methyl esters (FAMEs) through reaction with short-chain alcohols [11,12,13,14]. Although homogeneous alkaline catalysts exhibit high catalytic activity, their industrial application is limited by catalyst recovery difficulties, equipment corrosion, soap formation, and substantial wastewater generation [15,16,17]. In this context, heterogeneous catalysts have attracted increasing attention as more sustainable alternatives, offering simplified separation, catalyst reusability, and reduced environmental impact [18,19,20,21].

Among heterogeneous catalytic materials, calcium oxide (CaO) has been extensively investigated due to its strong basic character, low cost, and wide availability [22,23,24]. The catalytic behaviour of CaO is intrinsically associated with its ionic crystal structure, in which surface O^{2-} anions act as the primary Lewis basic sites responsible for methanol adsorption and activation during transesterification [24,25,26,27] (Fig. 1). More recently, the synthesis of CaO from biogenic residues, particularly eggshell waste, has emerged as a promising strategy for integrating catalyst development with circular economy principles [28,29,27,28]. Eggshell-derived CaO not only provides an environmentally attractive route for waste valorisation, but also has been reported to exhibit catalytic performance comparable to commercially available calcium-based materials in biodiesel synthesis [29,30,31].

Figure 1. Ionic crystal structure of calcium oxide (CaO), illustrating the spatial arrangement of Ca^{2+} and O^{2-} ions and the origin of surface basic sites associated with catalytic methanol activation.



Despite these advantages, unmodified CaO catalysts still present important limitations, including susceptibility to hydration and recarbonation, limited surface accessibility, and non-uniform distribution of catalytically active sites, which may compromise reaction efficiency and long-term performance [29,32,33,34]. To overcome these limitations, several surface

engineering strategies have been proposed, including the incorporation of alkaline species and transition metal oxides capable of modifying the structural, compositional, and catalytic properties of CaO-based systems [35,36,37,38,39].

Previous studies have demonstrated that surface modification can significantly improve biodiesel conversion efficiency [40,41,42,43]. However, most investigations have primarily focused on conversion yield, while the influence of catalyst modification on the balance between catalytic activity and product selectivity remains poorly understood [44,45,46,47]. In particular, the mechanisms by which different surface modifiers alter reaction kinetics, adsorption behaviour, and by-product suppression in waste-derived CaO catalysts remain insufficiently explored [29,48,49]. Furthermore, comparative studies involving waste-derived catalysts and commercial CaO under identical operating conditions are still limited, especially when non-conventional feedstocks are considered [50,27].

Coconut oil represents an attractive yet underexplored feedstock for biodiesel production due to its high content of medium-chain saturated fatty acids, which can significantly influence reaction kinetics, catalyst–substrate interactions, and ester formation behaviour [51,52,53,54,55]. Understanding how catalyst surface engineering affects transesterification performance in such systems may provide valuable insights for the rational design of next-generation sustainable catalysts [39,56,57,58].

Despite the extensive use of eggshell-derived CaO catalysts in biodiesel synthesis, most previous studies have primarily focused on conversion efficiency, with comparatively limited attention devoted to understanding how surface modification influences the balance between catalytic activity, product selectivity, and rate-controlling mechanisms under identical reaction conditions. Therefore, this study investigates the effect of KOH and ZnO surface modification on eggshell-derived CaO catalysts for coconut oil transesterification, using commercial CaO as a reference material. Particular emphasis is placed on understanding how chemical modification influences the activity–selectivity relationship, reaction kinetics, and physicochemical quality of the resulting biodiesel. By integrating structural characterisation, kinetic modelling, and fuel quality analysis, this work establishes a mechanistic framework for rationally tuning the catalytic behaviour of waste-derived CaO systems for sustainable biofuel production.

2. Materials and Methods

2.1 Materials

2.1.1 Eggshell waste collection

White chicken eggshells were collected from domestic consumption after the use of commercially purchased eggs obtained from a local market. The eggshell waste was used as precursor material for CaO synthesis through high-temperature calcination.

2.1.2 Coconut oil acquisition

Extra virgin coconut oil was commercially obtained from a local market and used as feedstock in the transesterification reactions. The fatty acid composition of the oil consisted of caproic acid (0.52%), caprylic acid (7.08%), capric acid (5.43%), lauric acid (46.58%), myristic acid (17.98%), palmitic acid (7.50%), stearic acid (2.86%), oleic acid (4.42%) and linoleic acid (0.65%).

2.1.3 Chemicals and reagents

The reagents used in this study were ethanol (C_2H_5OH, 99%, Synth), methanol (CH_3OH, 99.5%, Quimidrol), calcium oxide (CaO, 95%, ACS Científica), diethyl ether ($C_4H_{10}O$, 30–60 PA, Êxodo Científica), hydrochloric acid (HCl, 37%, Êxodo Científica), anhydrous sodium sulphate (Na_2SO_4, Dinâmica), sodium chloride (NaCl, 99%, Dinâmica), phenolphthalein ($C_{20}H_{14}O_4$, 99%, Êxodo Científica), potassium hydroxide (KOH, 85%, Dinâmica), zinc oxide (ZnO, 99%, Vetec Química Fina) and sodium hydroxide (NaOH) micropearls (98%, Dinâmica). All reagents were used as received without further purification.

2.2 Catalyst preparation

2.2.1 Synthesis of eggshell-derived CaO catalysts

Initially, the eggshells were subjected to a pre-treatment step involving washing with water and detergent in order to remove impurities and residual membranes adhered to the material. The cleaned shells were subsequently dried at room temperature for 24 h. Afterwards, the material was crushed, ground and sieved using an 80-mesh sieve, and the passing fraction was collected for further processing.

The obtained eggshell powder was calcined in a muffle furnace at 900 °C for 4 h, a condition previously reported as effective for the conversion of calcium carbonate ($CaCO_3$) into calcium oxide (CaO). The calcination process is represented by Eq. (1):

$$CaCO_3 \rightarrow CaO + CO_2 \quad (1)$$

2.2.2 Chemical modification of catalysts

The eggshell-derived CaO powder was separately modified with ZnO and KOH using a 1:1 mass ratio between CaO and the modifying agent, selected to ensure sufficient surface coverage and detectable incorporation of the modifying species during structural characterisation. Briefly, 5 mL of distilled water was added to 2 g of CaO powder in a porcelain crucible to promote homogeneous dispersion. Subsequently, 2 g of either ZnO or KOH was incorporated for the preparation of Zn-modified and K-modified catalysts, respectively.

The resulting mixtures were manually homogenised using a glass rod and dried at 120 °C for 2 h in order to remove physically adsorbed moisture and facilitate precursor fixation onto the CaO surface. Afterwards, the materials were calcined at 800 °C for 3 h to promote catalyst activation, decomposition of residual carbonate species, and stable incorporation of potassium- and zinc-containing surface phases into the CaO matrix.

2.2.3 Catalyst nomenclature

For a clearer discussion of the results, the catalysts were identified according to the nomenclature presented in Table 1.

Table 1. Nomenclature and abbreviations adopted for the catalyst samples.

Catalyst	Abbreviation
Eggshell	ES
Calcined eggshell	CES
ZnO-modified calcined eggshell	Zn-CES

KOH-modified calcined eggshell	K-CES

2.3 Catalyst characterisation

2.3.1 Scanning electron microscopy (SEM)

The morphology of the catalysts was investigated by scanning electron microscopy (SEM) using fourth-generation TESCAN microscopes.

2.3.2 X-ray diffraction (XRD)

The crystalline phases present in the catalysts were identified by X-ray diffraction (XRD) using a Bruker D2 Phaser diffractometer equipped with a LynxEye detector and CuKα radiation (λ = 1.54 Å). The analyses were performed using nickel-filtered radiation at 30 kV and 10 mA. Diffractograms were recorded over a 2θ range of 3–70°, with a step size of 0.02°, acquisition time of 0.1 s, divergent slit of 0.6 mm and central slit of 1 mm.

2.3.3 Fourier transform infrared spectroscopy (FTIR)

FTIR analyses were performed to identify the functional groups present in the catalysts. Spectra were obtained using an IRAffinity-1 Fourier Transform Infrared Spectrophotometer (Shimadzu) equipped with an attenuated total reflectance (ATR) accessory over the range of 4000–400 cm^{-1} with a resolution of 4 cm^{-1}. Additional analyses were carried out using a BRUKER FT-IR VERTEX 70 spectrometer operating within the range of 500–4000 cm^{-1} and resolution of 4 cm^{-1}. All spectra were recorded in transmittance mode.

2.3.4 Thermogravimetric analysis (TG/DTG)

Thermogravimetric analyses were performed using a TG 209 F3 Tarsus analyser (NETZSCH) equipped with a platinum crucible. The experiments were conducted from 30 to 900 °C at a heating rate of 10 °C min^{-1} under nitrogen atmosphere with a flow rate of 20 mL min^{-1} in order to evaluate the thermal stability and mass loss behaviour of the catalysts.

2.3.5 X-ray fluorescence (XRF)

The elemental composition of the catalysts was determined by X-ray fluorescence (XRF) using a BRUKER S2 PUMA SERIES II spectrometer equipped with a Pd tube operating at a maximum power of 50 W, voltage of 50 kV and current of 1 mA, coupled with a HighSense Silicon Drift Detector (HighSense SDD).

2.4 Biodiesel production

Biodiesel was produced using 20 g of coconut oil, previously heated at 60 °C for 20 min under stirring at 750 rpm in order to remove residual moisture. Transesterification reactions were carried out in a round-bottom flask under magnetic stirring at 750 rpm using 1.5 wt% catalyst and a methanol-to-oil molar ratio of 19:1. After addition of the oil, the reaction proceeded at 64 °C.

At the end of the reaction, the mixture was transferred to a separating funnel and allowed to stand for 24 h to promote phase separation. Subsequently, glycerol and catalyst residues were removed.

The crude biodiesel was purified by washing with 50 mL of 0.5 M HCl solution for 30 min, followed by the addition of saturated NaCl solution and a further decantation step. The biodiesel was then dried using 0.5 g of anhydrous Na_2SO_4 under stirring for 30 min. Finally, the product was filtered and weighed to determine biodiesel yield.

Biodiesel yield was calculated according to Eq. (2):

$$\text{Biodiesel yield (\%)} = \frac{Mass\ of\ biodiesel\ obtained\ (g)}{Mass\ of\ oil\ used\ (g)} \times 100 \quad (2)$$

2.5 Kinetic Modeling of the Transesterification Reaction

2.5.1 Pseudo-First-Order Kinec Model

The transesterification reaction for biodiesel production from waste cooking oil has been extensively investigated using heterogeneous catalysts. Gupta and Rathod [59] evaluated the use of eggshell-derived catalysts in the transesterification of residual frying oil. In this process, one mole of triglycerides (TG) reacts with three moles of methanol (MeOH) to produce three moles of fatty acid methyl esters (FAME) and one mole of glycerol, as represented in Equation 3.

$$TG + 3MeOH \rightleftharpoons 3FAME + Glycerol \quad (3)$$

The overall reaction rate for the transesterification process can be expressed by Equation 4:

$$-rA = -\frac{d[TG]}{dt} = K_0[TG][MeOH]^3 \quad (4)$$

Where [TG] and [MeOH] represent the molar concentrations ($mol \cdot L^{-1}$) of triglycerides and methanol, respectively, and k_0 is the kinetic rate constant.

Since the transesterification reaction is reversible, an excess amount of methanol is generally employed to shift the equilibrium toward product formation. Under these conditions, the methanol concentration remains approximately constant during the reaction, allowing the kinetic model to be simplified to a pseudo-first-order reaction [60].

According to Yingying *et al*. [60], the following assumptions are considered for the pseudo-first-order approach:

i) the reaction system behaves as pseudo-homogeneous under high stirring conditions;

ii) triglycerides, diglycerides, and monoglycerides are not distinguished in the global reaction mechanism;

iii) methanol concentration remains constant due to its large molar excess.

Based on these assumptions, Equation 4 can be simplified as follows:

$$-rA = -\frac{d[TG]}{dt} = k[TG] \quad (5)$$

where:

$$\boldsymbol{k = k_0 [MeOH]^3} \quad (6)$$

Integrating Equation 7 between the initial triglyceride concentration $[TG]_0$ at t=0 and the triglyceride concentration [TG] at time t, Equation 7 is obtained:

$$ln[TG]_0 - ln[TG] = kt \quad (7)$$

Expressing the equation in terms of triglyceride conversion (X_A), the kinetic model can be rewritten as:

$$-ln(1 - X_A) = kt \quad (8)$$

2.5.2 Pseudo-Second-Order Kinetic Model

The transesterification reaction has also been described using a pseudo-second-order kinetic model. Feyzi and Khajavi [61] evaluated this approach considering the reaction kinetics under excess methanol conditions.

For the pseudo-second-order model, the following assumptions were adopted:

i) the overall transesterification reaction follows second-order kinetics;

ii) due to the high methanol-to-oil molar ratio, the reaction rate depends only on the oil concentration;

iii) the reverse reaction can be neglected because of the excess methanol and the low concentration of reaction products;

iv) the oil and methanol phases are perfectly mixed, allowing uniform composition throughout the reaction medium.

Under these assumptions, the reaction rate can be expressed by Equation 9:

$$-rA = -\frac{dC_A}{dt} = k_2 C_A^2 \quad (9)$$

Where CA is the oil concentration and k_2 is the pseudo-second-order kinetic constant. After integration of Equation 10 in terms of conversion, Equation 10 is obtained:

$$\frac{1}{1 - X_A} = k_2 C_{A0} t \quad (10)$$

The linear relationship between $\frac{1}{1-X_A}$ and reaction time allows determination of the kinetic parameter $k_2 C_{A0}$ from the slope of the fitted line. Considering a constant initial oil concentration, the transesterification kinetic constant can therefore be estimated [61].

2.6 Biodiesel characterisation

2.6.1 Fourier transform infrared spectroscopy (FTIR)

FTIR analyses of coconut oil and biodiesel samples were performed using an IRAffinity-1 spectrophotometer (Shimadzu) equipped with an ATR accessory within the range of 4000–400 cm^{-1} and resolution of 4 cm^{-1}. Spectra were obtained in transmittance mode.

2.6.2 Thermogravimetric analysis (TG/DTG)

Thermogravimetric analyses of coconut oil and biodiesel samples were performed using a TG 209 F3 Tarsus analyser (NETZSCH). The experiments were conducted from 30 to 900 °C at a heating rate of 10 °C min^{-1} under nitrogen atmosphere with a flow rate of 20 mL min^{-1} using platinum crucibles.

2.6.3 Gas chromatography with flame ionisation detection (GC-FID)

The biodiesel composition was determined by gas chromatography coupled with flame ionisation detection (GC-FID) using a GC-2010 Plus AF chromatograph equipped with a DB-5 capillary column (30 m × 0.25 mm × 0.25 μm; 5% diphenyl/95% dimethylpolysiloxane, Agilent).

The oven temperature programme was set from 130 to 200 °C at 12 °C min^{-1}, followed by heating from 200 to 215 °C at 4 °C min^{-1} and from 215 to 250 °C at 4 °C min^{-1}, maintaining the final temperature for 2 min, resulting in a total run time of 20.33 min. The injection volume was 1 μL with a split ratio of 1:50. Injector and detector temperatures were maintained at 220 and 260 °C, respectively, under a pressure of 100 kPa using nitrogen as carrier gas.

Sample preparation followed the EN 14103 standard. Briefly, 100 mg of sample was diluted in a 10 mL volumetric flask using n-hexane. Subsequently, 200 μL of this solution was transferred to a 1 mL volumetric flask, followed by the addition of 50 μL of internal standard solution (methyl heptadecanoate, 5000 mg L^{-1}), and the volume was completed with n-hexane prior to injection.

The ester content was calculated according to Eq. (3):

$$\%\,Esters = \left(\frac{\Sigma A - API}{API} \times \frac{CPI}{Csample}\right) \times 100 \quad (3)$$

where ΣA corresponds to the sum of the peak areas of the major biodiesel components and the internal standard, API is the peak area of the internal standard, CPI is the concentration of the internal standard, and Csample is the concentration of the injected sample.

2.6.4 Viscosity and density

Kinematic viscosity and density measurements were performed using an SVM 3000 viscometer (Anton Paar).

4. Results and Discussion

4.1 Catalyst characterisation

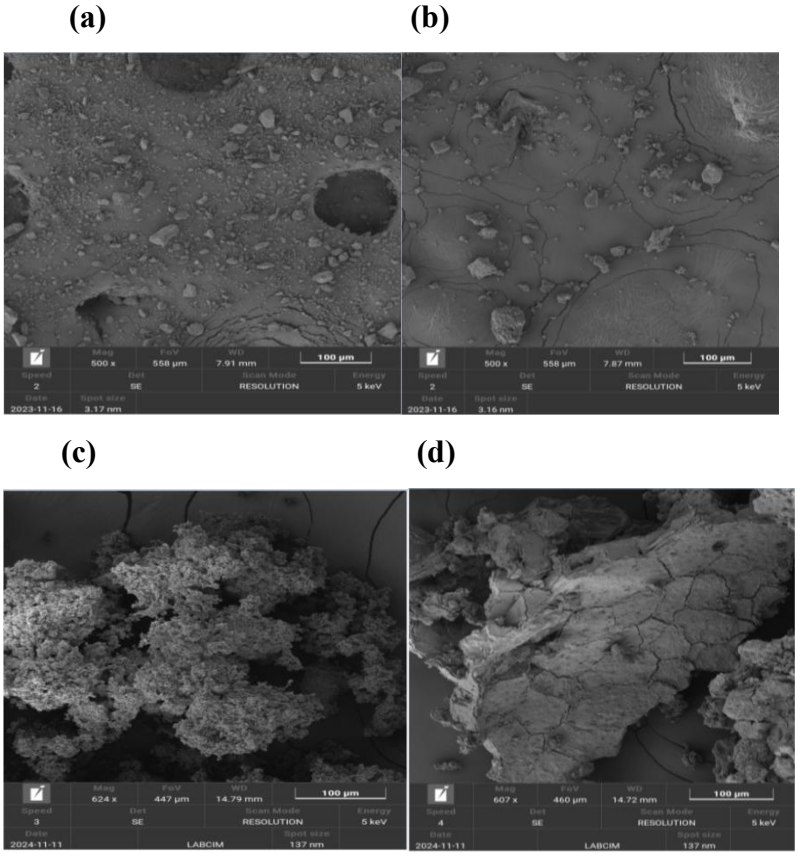
The characterisation of the eggshell-derived catalysts revealed significant structural, morphological, compositional and thermal changes after calcination and chemical modification, as evidenced by SEM, XRD, FTIR, XRF, TG/DTG and EDS analyses. These modifications appear to be closely associated with catalytic performance, since they influence the availability, distribution, and physicochemical nature of catalytically active surface environments [61,62,63,64].

4.1.1 Scanning electron microscopy (SEM)

SEM micrographs of ES, CES, Zn–CES, and K–CES are presented in Fig. 2. The ES sample (Fig. 2a) exhibited particles with heterogeneous sizes, irregular morphology, and a poorly organised surface, indicating low structural uniformity [65,66]. After calcination (Fig. 2b), a marked morphological reorganisation was observed, with the formation of a more homogeneous and interconnected structure, which can be associated with CO_2 release during $CaCO_3$ decomposition and the consequent formation of CaO [67,68].

Additional surface modifications were observed after chemical treatment. The Zn–CES sample (Fig. 2c) showed finer particles with partial agglomeration, suggesting the deposition of Zn-containing species on the CaO surface [69,70]. In contrast, K–CES (Fig. 2d) exhibited denser agglomerates and a more compact surface, possibly due to the formation of potassium-containing surface species during calcination [71]. Overall, calcination and chemical modification significantly altered the surface morphology of the catalysts, which may affect active-site distribution and catalytic performance during the transesterification reaction [72,73].

Figure 2. SEM micrographs of (a) ES, (b) CES, (c) Zn–CES, and (d) K–CES samples.

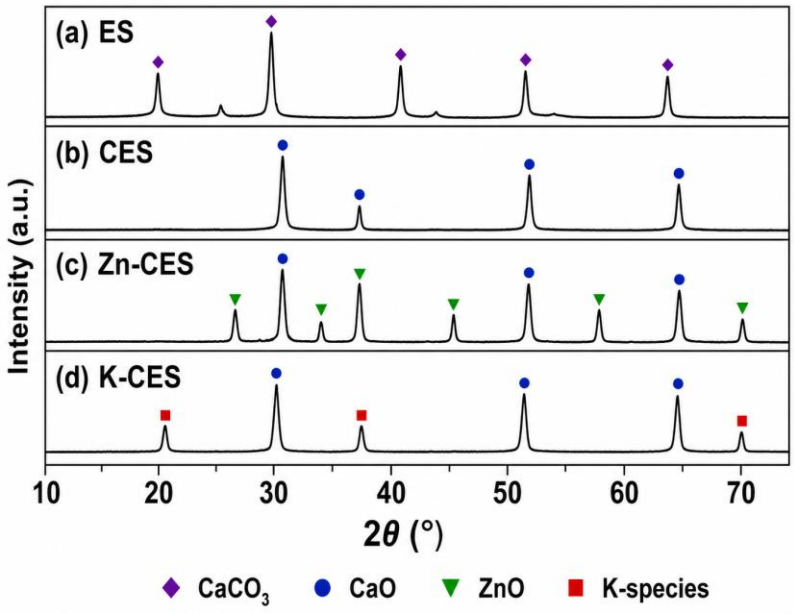


4.1.2 X-ray diffraction (XRD)

The X-ray diffraction patterns of ES, CES, Zn-CES, and K-CES are shown in Fig. 3. The raw eggshell (ES) exhibited characteristic reflections of crystalline $CaCO_3$ (calcite), confirming the typical mineral composition of the precursor material [74,75,76]. After calcination, the diffraction profile of CES changed markedly, with the disappearance of calcite reflections and the emergence of characteristic peaks of cubic CaO, indicating the successful thermal decomposition of $CaCO_3$ and the formation of a highly crystalline CaO phase [77,78,79]. After zinc modification, additional reflections corresponding to hexagonal ZnO (wurtzite) were observed in Zn-CES, corroborating the successful incorporation of zinc species into the catalyst matrix [80,81,82]. Similarly, the diffraction pattern of K-CES exhibited additional reflections associated with potassium-containing crystalline species formed during the calcination of the KOH-impregnated support, confirming the effective potassium modification [83,84,85]. Overall, the XRD results demonstrate the structural evolution from the raw precursor (ES) to calcined CaO (CES), followed by the successful incorporation of Zn and K species in Zn-CES and K-CES, respectively. These structural modifications may

contribute to changes in surface basicity and active-site distribution, potentially enhancing catalytic performance during the transesterification reaction [80,81,82,84,85].

Figure 3. XRD patterns of (a) ES, (b) CES, (c) Zn-CES, and (d) K-CES samples.



4.1.3 Fourier transform infrared spectroscopy (FTIR)

The FTIR spectra of ES, CES, Zn–CES, and K–CES are shown in Fig. 4. The ES sample exhibited characteristic absorption bands at approximately 2506, 1798, 1395, 1083, 872, and 712 cm^{-1}, which are assigned to carbonate vibrations of calcite ($CaCO_3$), confirming the typical mineral composition of the raw eggshell [86,87]. A weak band near 3641 cm^{-1} was attributed to O–H stretching vibrations [88,89]. After calcination, the spectra of CES showed a marked reduction in carbonate-related bands, indicating the thermal decomposition of $CaCO_3$ and the formation of CaO [89,90], in agreement with the XRD results. The absorption bands observed near 3614 cm^{-1} suggest partial surface hydroxylation due to moisture adsorption, which is commonly reported for CaO-based materials [88,89]. The modified catalysts (Zn–CES and K–CES) exhibited spectral profiles similar to CES, indicating that the main structural features of CaO were preserved after chemical modification. Minor variations in the intensity of hydroxyl and carbonate bands suggest changes in the surface chemical environment after Zn and K incorporation, which may influence the basicity and catalytic performance during the transesterification reaction [90,91,92].

Figure 4. FTIR spectra of (a) ES, (b) CES, (c) Zn–CES, and (d) K–CES samples.

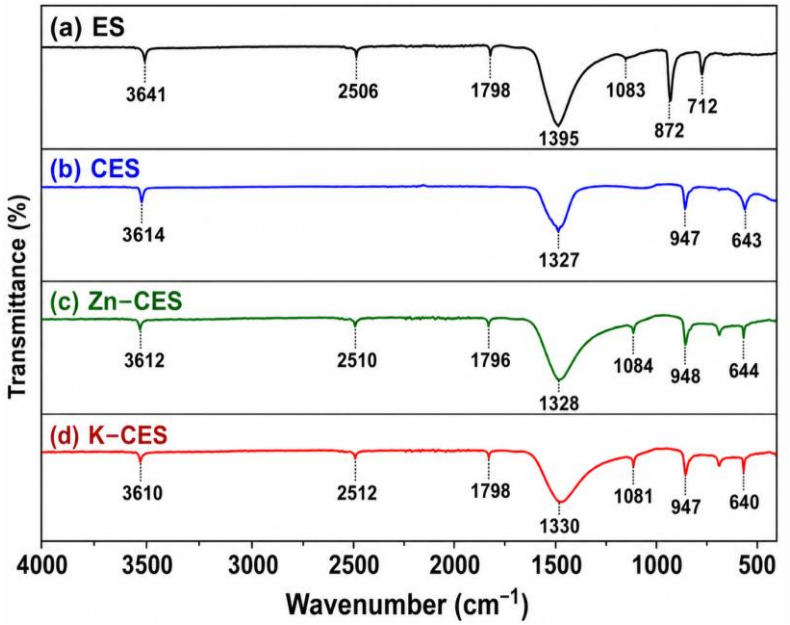


Table 2. FTIR results for the catalysts.

Wavenumber (cm^{-1})	Assignment	Functional Group
3641	O–H stretching	$Ca(OH)_2$
3614 (Zn) / 3610 (K)	O–H stretching	Adsorbed hydroxyl groups
2521–2506	CO_3^{2-} vibrations	$CaCO_3$
1798–1785	CO_3^{2-} vibrations	$CaCO_3$
1450–1395	Asymmetric vibration of CO_3^{2-}	$CaCO_3$
1227–1228	Asymmetric stretching of CO_3^{2-}	$CaCO_3$ in modified structure
1083–1080	Characteristic calcite vibration	$CaCO_3$
872–709	Out-of-plane vibrations and bending modes of CO_3^{2-}	$CaCO_3$

867	CO_3^{2-} bending	$CaCO_3$ associated with Zn
643 and 631	CO_3^{2-} bending modes	$CaCO_3$

4.1.4 X-ray fluorescence (XRF)

The chemical composition of ES, CES, Zn–CES, and K–CES, determined by X-ray fluorescence (XRF), is presented in Table 2. The CES sample exhibited a high CaO content (98.29 wt.%), confirming the effectiveness of the calcination process and the efficient conversion of $CaCO_3$ into catalytically active CaO. After chemical modification, the successful incorporation of Zn and K species was clearly observed. The Zn–CES catalyst contained 47.56 wt.% Zn, while K–CES showed 5.54 wt.% K, confirming the effectiveness of the impregnation procedure. A concomitant reduction in Ca content was observed after modification, suggesting partial surface coverage of CaO by the incorporated species. These results are consistent with the structural and spectroscopic analyses and indicate that Zn and K incorporation may modify the surface basicity and catalytic behaviour of the eggshell-derived catalysts during the transesterification reaction [93,94].

Table 2. Chemical composition of ES, CES, Zn–CES, and K–CES samples determined by X-ray fluorescence (XRF).

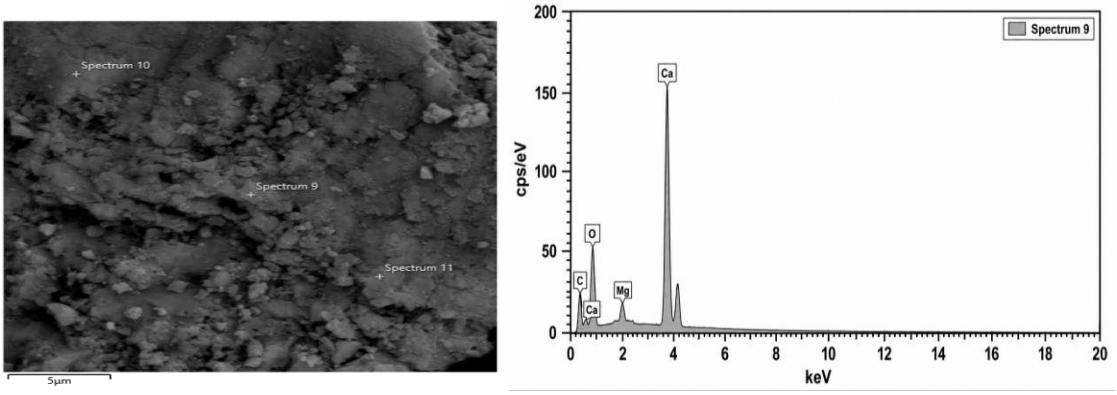
Sample	CaO (wt.%)	ZnO (wt.%)	K_2O (wt.%)	SrO (wt.%)	SO_3 (wt.%)	Al_2O_3 (wt.%)	Others (wt.%)
ES	98.89	–	–	0.41	0.30	0.09	0.31
CES	98.29	–	–	0.26	0.28	0.10	1.07
Zn–CES	51.31	47.56	–	0.18	0.03	0.10	0.82
K–CES	92.36	–	5.54	0.23	0.01	0.34	1.52

4.1.5 Energy-dispersive X-ray spectroscopy (EDS)

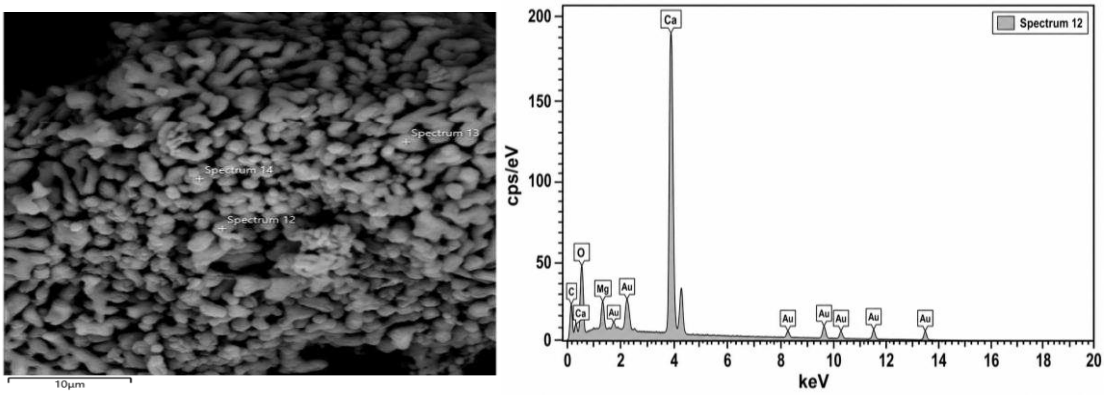
The EDS spectra of ES, CES, Zn–CES, and K–CES are presented in Fig. 5. The elemental compositions corroborated the XRF and XRD results, confirming Ca as the major constituent of all samples. After calcination, a marked reduction in carbon content was observed in CES, indicating the thermal decomposition of $CaCO_3$ and the formation of CaO [95,96]. The modified catalysts exhibited additional Zn and K signals in Zn–CES and K–CES, respectively, confirming the successful incorporation of the modifying species after chemical treatment [97,. These compositional changes are consistent with the structural and spectroscopic analyses and suggest modifications in the surface chemical environment, which may influence the catalytic behaviour of the eggshell-derived catalysts during the transesterification reaction.

Figure 5. EDS spectra of (a) ES, (b) CES, (c) Zn–CES, and (d) K–CES samples.

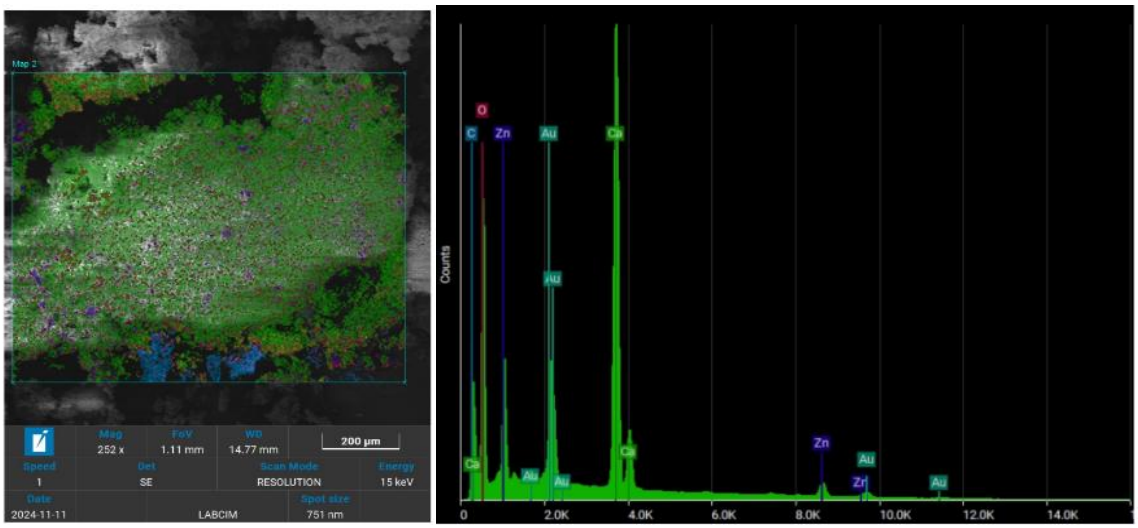
(a)

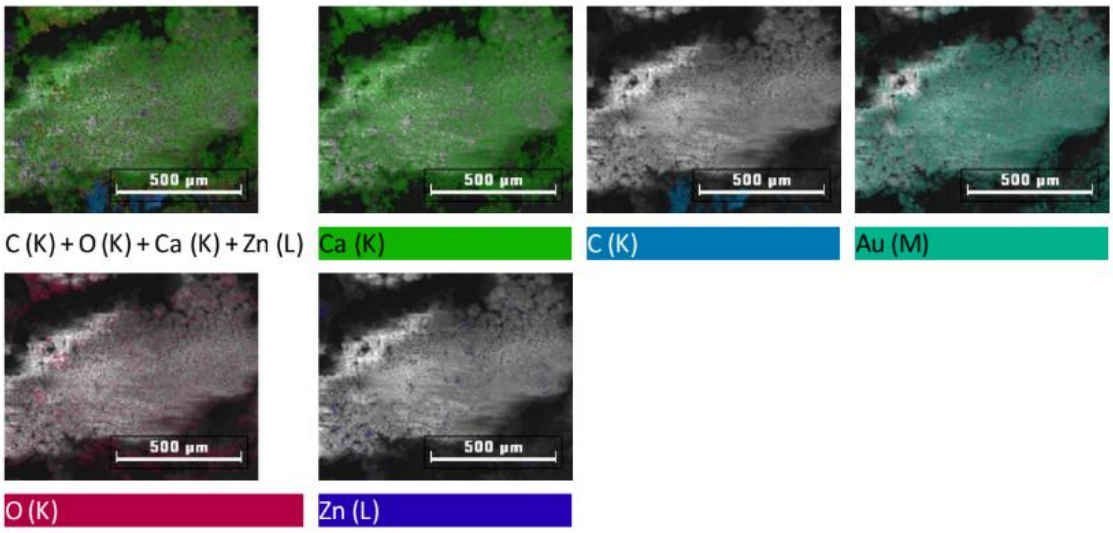


(b)

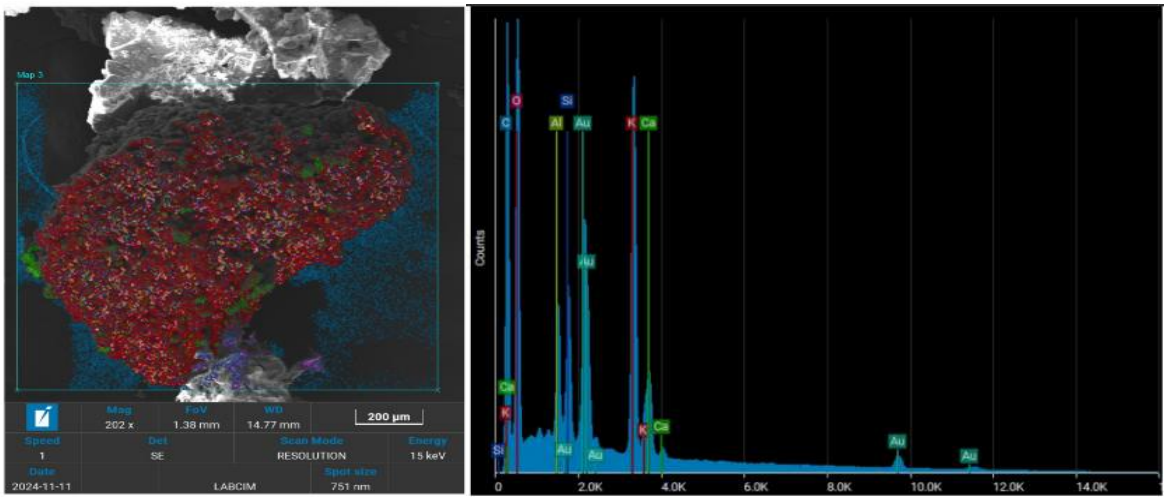


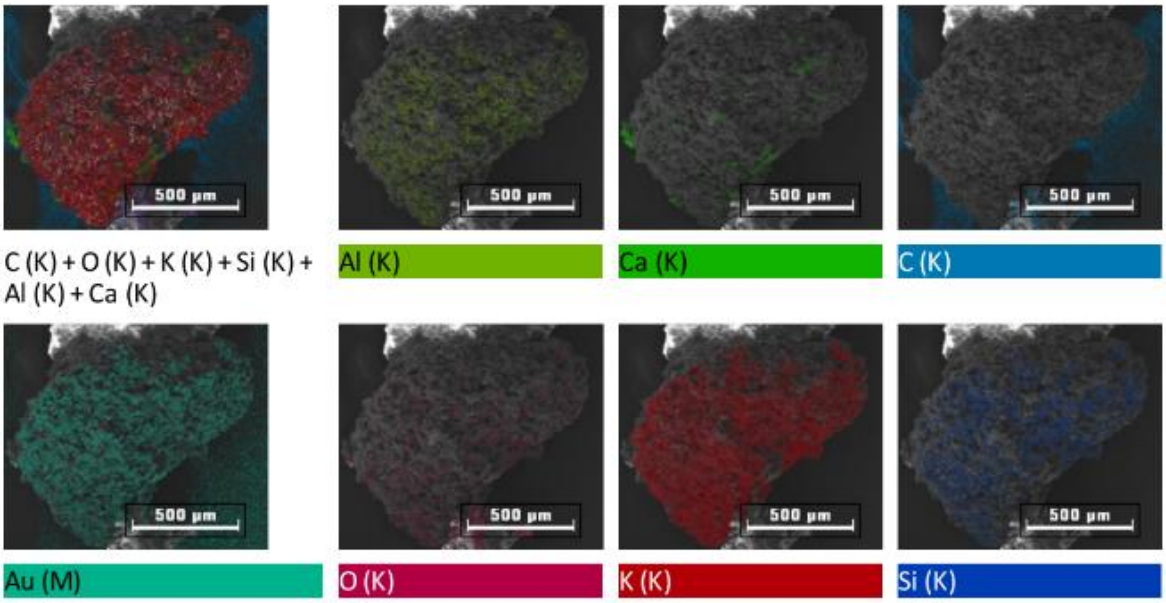
(c)


Map 3
Mag 252 x
FoV 1.11 mm
WD 14.77 mm
200 µm
Speed 1
Det SE
Scan Mode RESOLUTION
Energy 15 keV
Date 2024-11-11
LABCIM
Spot size 751 nm
O
C
Zn
Au
Ca
Counts
0
2.0K
4.0K
6.0K
8.0K
10.0K
12.0K
14.0K


500 µm
C (K) + O (K) + Ca (K) + Zn (L)
Ca (K)
C (K)
Au (M)
O (K)
Zn (L)

(d)

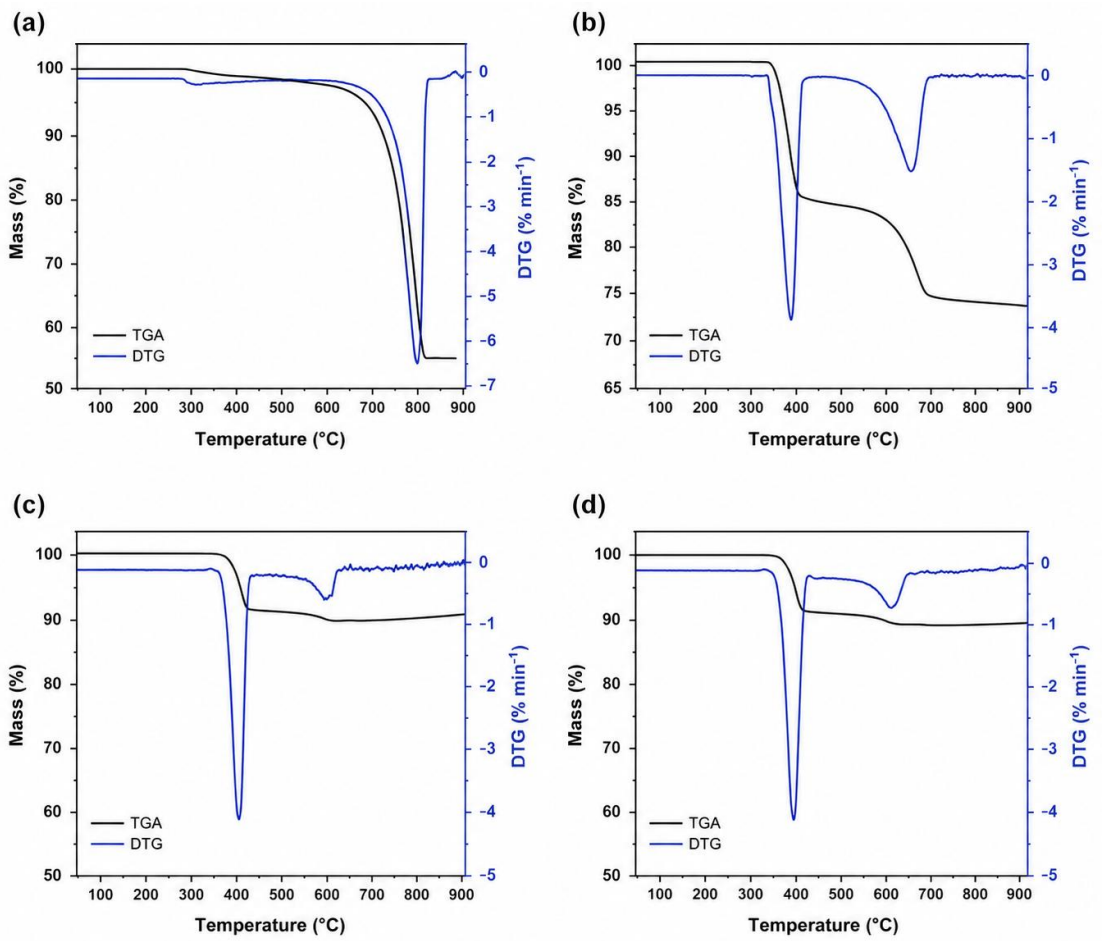

Map 3
Mag 202 x
FoV 1.38 mm
WD 14.77 mm
200 µm
Speed 1
Det SE
Scan Mode RESOLUTION
Energy 15 keV
Date 2024-11-11
LABCIM
Spot size 751 nm
O
Si
C
Al
Au
K
Ca
Counts
0
2.0K
4.0K
6.0K
8.0K
10.0K
12.0K
14.0K



4.1.6 Thermogravimetric analysis (TG/DTG)

The TG/DTG curves of ES, CES, Zn–CES, and K–CES are shown in Fig. 6. The ES sample exhibited a pronounced mass loss associated with the thermal decomposition of $CaCO_3$ and the release of CO_2, confirming the carbonate nature of the raw precursor. After calcination, CES showed significantly improved thermal stability, with only minor residual mass losses, which may be associated with partial surface hydration or recarbonation after exposure to atmospheric moisture and CO_2. The modified catalysts (Zn–CES and K–CES) exhibited lower mass losses and higher residual masses compared with CES, indicating enhanced thermal stability after chemical modification. Overall, the TG/DTG results confirm the effective conversion of $CaCO_3$ into CaO after calcination and demonstrate that Zn and K incorporation altered the thermal behaviour of the eggshell-derived catalysts, which may influence catalyst stability and surface reactivity during the transesterification reaction.

Figure 6. TG and DTG curves of (a) ES, (b) CES, (c) Zn–CES, and (d) K–CES samples.



4.2 Catalytic performance in transesterification

4.2.1 Effect of catalyst modification on biodiesel yield

The catalytic performance of CES, Zn–CES, and K–CES was evaluated in the transesterification of coconut oil under identical reaction conditions. The results obtained are presented in Table 3 and Fig. 7, where all catalysts showed a progressive increase in biodiesel yield with reaction time, indicating the contribution of both reaction kinetics and mass-transfer phenomena. The unmodified catalyst (CES) exhibited moderate catalytic activity, reaching a maximum biodiesel yield of 66.3% after 120 min, suggesting that calcination alone was insufficient to maximise catalytic performance. In contrast, K–CES showed the highest catalytic activity, achieving a biodiesel yield of 86.9%, comparable to commercial CaO (86.4%). This enhanced performance can be associated with the incorporation of potassium species, which may increase surface basicity and promote methoxide formation during

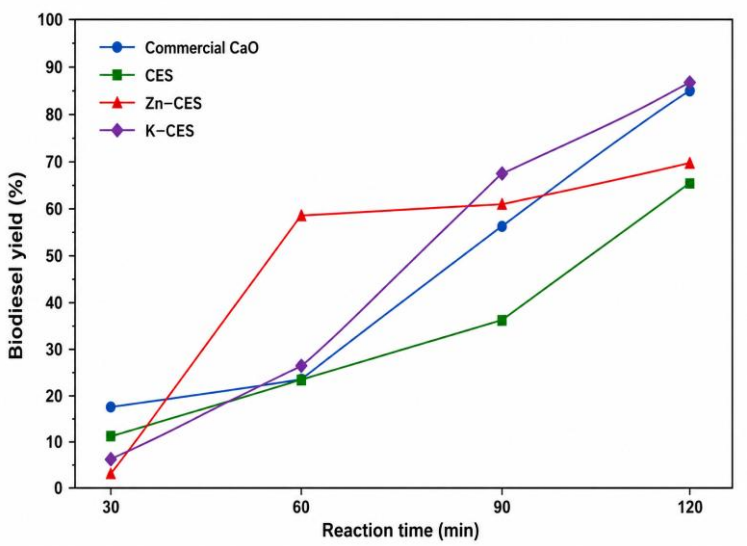
transesterification. The Zn–CES catalyst reached an intermediate biodiesel yield (70.35%), but exhibited the highest ester content (98.1%), suggesting improved selectivity towards the transesterification reaction. This behaviour indicates that Zn incorporation may alter catalyst–substrate interactions and suppress parallel reactions, such as saponification. Overall, catalyst modification significantly influenced both catalytic activity and selectivity, demonstrating that Zn and K incorporation can effectively tailor the catalytic behaviour of eggshell-derived CaO catalysts for biodiesel production.

Table 3. Biodiesel yield obtained during coconut oil transesterification using commercial

Catalyst	30 min (%)	60 min (%)	90 min (%)	120 min (%)
Commercial CaO	17.7	22.8	55.7	86.4
CES	11.2	24.6	36.5	66.3
Zn–CES	5.4	59.4	60.9	70.35
K–CES	7.4	26.8	67.5	86.9

CaO and eggshell-derived catalysts.

Figure 7. Effect of reaction time on biodiesel yield during transesterification reactions using commercial CaO and eggshell-derived catalysts.



4.2.2 Activity–selectivity relationship

Although K–CES achieved the highest biodiesel yield, Zn–CES exhibited the highest ester content (98.1%), indicating a clear trade-off between catalytic activity and selectivity. Importantly, high gravimetric yield did not necessarily correspond to high ester purity, suggesting the co-extraction of residual glycerides, soaps, or partially converted intermediates in some catalytic systems. This finding indicates that catalyst modification influenced not only triglyceride conversion, but also the chemical composition and selectivity of the final biodiesel product. The superior catalytic activity of K–CES can be associated with the presence of potassium-containing species, which may enhance surface basicity, promote methoxide formation, and accelerate triglyceride conversion. However, highly basic catalytic sites may also favour parallel reactions, particularly saponification, which can negatively affect product selectivity. In contrast, Zn incorporation appears to provide a more selective catalytic environment, favouring transesterification while suppressing secondary reactions. These results demonstrate that catalyst modification can be strategically used to tailor either catalytic activity or biodiesel quality, depending on the desired process objective. To the best of our knowledge, comparative evidence demonstrating an experimentally resolved activity–selectivity trade-off in chemically modified eggshell-derived CaO catalysts under identical transesterification conditions remains scarcely reported.

4.2.3 Comparison with literature

To benchmark the catalytic performance obtained in this study, Table 4 compares the reaction conditions and biodiesel yields reported for eggshell-derived CaO catalysts in previous studies. The results show that K–CES achieved biodiesel yields comparable to those reported for other modified CaO-based catalysts, despite the lower catalyst loading employed in this work. In addition, Zn–CES exhibited excellent ester purity, demonstrating that chemical modification effectively tailored catalyst selectivity. These findings highlight the potential of the proposed eggshell-derived catalysts as efficient and competitive materials for biodiesel production.

Table 4. Comparison of reaction conditions and catalytic performance of eggshell-derived CaO catalysts reported in the literature and in the present study.

Catalyst	**Feedstock**	**Alcohol/oil ratio**	**Catalyst loading (wt.%)**	**Temperature (°C)**	**Time (min)**	**Biodiesel yield (%)**	**Ester content (%)**	**Reference**
Eggshell CaO	Sunflower oil	9:1	3.0	65	120	90.1% (pink eggshells) and 92.8% (green eggshells)	—	Graziottin *et al*. (2020)
Eggshell CaO	Marine fish waste oil	25:1	5.0	57	107	86.5	—	Karkal and Kudre (2023)
Zn/CaO derived from eggshells	Waste cooking oil	15:1	4.0	65	150	94.1	—	Rahman *et al*. (2021)
Commercial CaO	Coconut oil	19:1	1.5	64	120	86.0	60.56	This work

CES	Coconut oil	19:1	1.5	64	120	66.3	63.51	This work
K–CES	Coconut oil	19:1	1.5	64	120	86.9	74.06	This work
Zn–CES	Coconut oil	19:1	1.5	64	120	70.3	98.1	This work

4.3 Kinetic modelling of the transesterification reaction

Although simplified pseudo-order models do not fully capture the complexity of heterogeneous transesterification systems, they provide useful comparative descriptors for evaluating changes in catalyst-dependent rate behaviour under fixed operating conditions.

4.3.1 Pseudo-first-order model

The kinetic analysis showed that the pseudo-first-order model adequately described the transesterification behaviour of K–CES, as shown in Fig. 8. This catalyst exhibited the highest correlation coefficient ($R^2 = 0.947$) and a kinetic constant of 0.0223 min^{-1} (Table 5), indicating that the reaction was predominantly controlled by the chemical reaction step under the evaluated conditions. In comparison, CES exhibited lower kinetic constant values, reflecting its reduced catalytic activity. The commercial CaO catalyst also showed satisfactory agreement with the pseudo-first-order model, although with lower correlation coefficients than K–CES. These results are consistent with the physicochemical characterisation, suggesting that potassium incorporation may have enhanced the density or accessibility of catalytically active basic environments.

Figure 8. Pseudo-first-order kinetic model for coconut oil transesterification using commercial CaO, CES, Zn–CES, and K–CES catalysts.

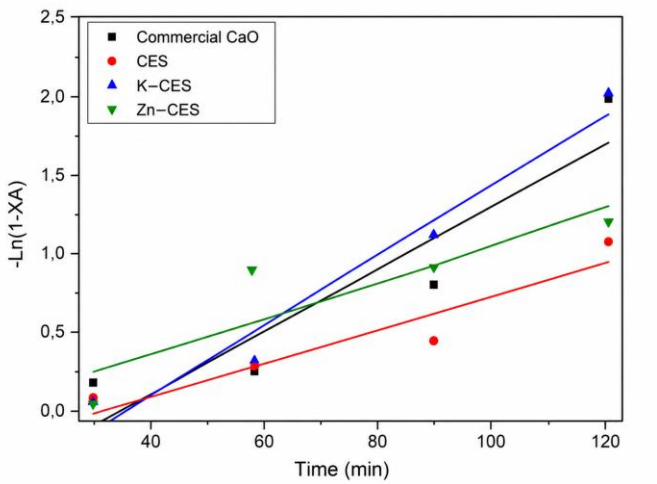


Table 5. Kinetic parameters obtained from the pseudo-first-order model.

Catalyst	Linear equation	k (min^{-1})	R^2
Commercial CaO	y = 0.0199x − 0.673	0.0199	0.850
CES	y = 0.0103x − 0.284	0.0103	0.879
Zn–CES	y = 0.0117x − 0.102	0.0117	0.820
K–CES	y = 0.0223x − 0.783	0.0223	0.947

4.3.2 Pseudo-second-order model

The pseudo-second-order model provided the best fit for Zn–CES, which exhibited a correlation coefficient of 0.894 and a kinetic constant of 0.0235 min^{-1} (Table 6), as shown in Fig. 9. This behaviour suggests a greater contribution of surface interactions and adsorption phenomena during the transesterification reaction. The differences observed between the kinetic models indicate that catalyst modification not only affected reaction rates, but also influenced the dominant reaction pathway and the rate-controlling step. While K–CES showed behaviour consistent with a pseudo-first-order mechanism, Zn–CES exhibited better agreement with the pseudo-second-order model, suggesting distinct catalytic environments after chemical modification.

Figure 9. Pseudo-second-order kinetic model for coconut oil transesterification using commercial CaO, CES, Zn–CES, and K–CES catalysts.

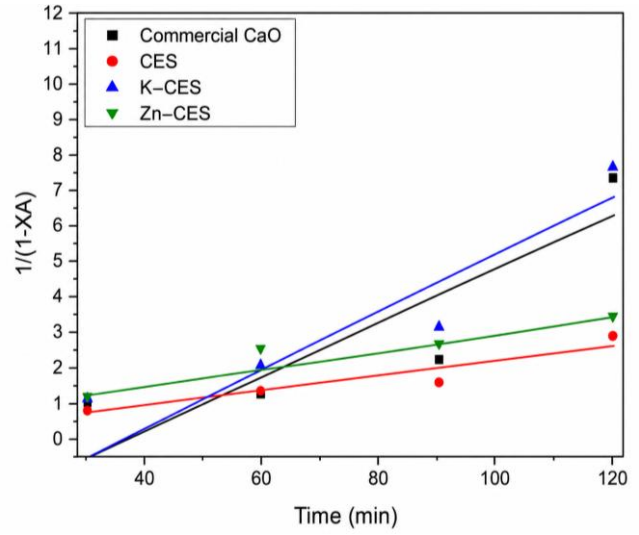


Table 6. Kinetic parameters obtained from the pseudo-second-order model.

Catalyst	Linear equation	k (min^{-1})	R^2
Commercial CaO	y = 0.0646x − 1.81	0.0646	0.734
CES	y = 0.0192x + 0.306	0.0192	0.800
Zn–CES	y = 0.0235x + 0.602	0.0235	0.894
K–CES	y = 0.0712x − 2.05	0.0712	0.831

4.3.3 Mechanistic implications

The kinetic results confirmed that chemical modification significantly influenced both catalytic activity and reaction mechanism. K–CES exhibited behaviour characteristic of a reaction-controlled system, which can be associated with enhanced surface basicity and rapid methoxide formation. In contrast, Zn–CES showed a greater dependence on adsorption and interfacial interactions, suggesting that Zn incorporation may alter the rate-controlling step of the transesterification reaction. These findings further support the trade-off between catalytic activity and selectivity observed for the modified CaO-based catalysts. Overall, the incorporation of K and Zn enabled the tuning of catalytic behaviour according to process requirements, either maximising biodiesel yield (K–CES) or improving ester purity and reaction selectivity (Zn–CES).

4.4 Biodiesel characterisation

4.4.1 FTIR spectra of biodiesel

The FTIR spectra of the biodiesel samples are presented in Fig. 10, and the main band assignments are summarised in Table 7. All samples exhibited the characteristic absorption bands of fatty acid methyl esters (FAME), confirming the efficient conversion of coconut oil into biodiesel. The intense band at approximately 1739 cm^{-1} corresponds to ester carbonyl (C=O) stretching, while the bands near 2923 and 2850 cm^{-1} are associated with aliphatic C–H stretching. Additional bands at approximately 1461, 1165, and 717 cm^{-1} further confirmed methyl ester formation. The biodiesel samples obtained using Zn–CES and K–CES exhibited similar spectroscopic profiles, with slight variations in band intensity, suggesting differences in conversion efficiency and product composition, consistent with the catalytic performance and ester content previously discussed. Overall, the FTIR results confirmed the formation of high-quality biodiesel for all catalytic systems.

Figure 10. FTIR spectra of biodiesel samples produced from coconut oil using commercial CaO, CES, Zn–CES, and K–CES catalysts.

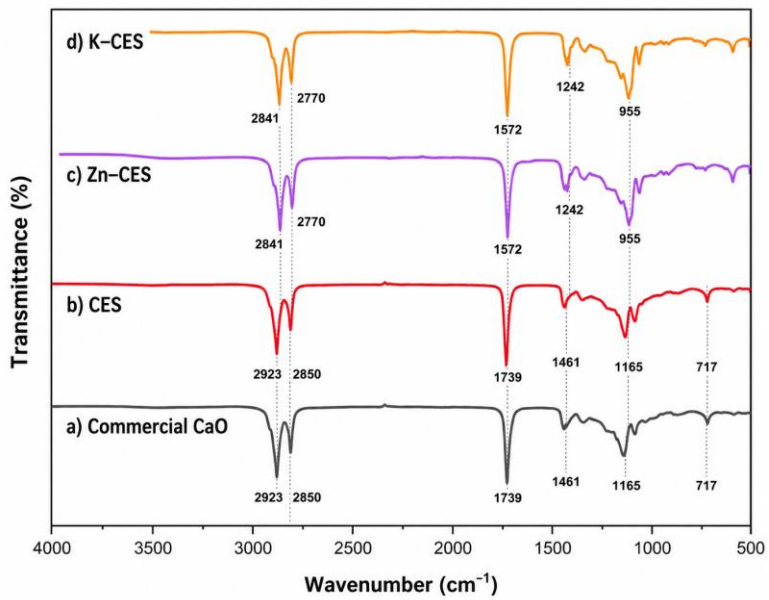


Table 7. Main FTIR absorption bands and assignments of biodiesel samples produced using the different catalytic systems.

Wavenumber (cm^{-1})	Assignment	Functional group

2923–2850	ν(C–H)	CH_2 / CH_3 (aliphatic chains)
2841–2770	ν(C–H)	Aliphatic hydrocarbons
1739	ν(C=O)	Ester carbonyl
1572	ν(C=C)	Unsaturated bonds
1461	δ(C–H)	Aliphatic groups
1242–1165	ν(C–O)	Ester groups
955	γ(C–H)	Unsaturated structures
717	γ(C–H)	Long-chain hydrocarbons

4.4.2 Thermogravimetric analysis (TGA/DTG)

The TG/DTG curves of the biodiesel samples are presented in Fig. 11, and the main thermal events are summarised in Table 8. All samples exhibited thermal decomposition profiles characteristic of fatty acid methyl esters (FAME), with the main mass-loss events occurring between approximately 90 and 410 °C. The biodiesel produced using CES showed two degradation stages, with the main decomposition occurring between 285.78 and 410.78 °C and a low residual mass (0.50 wt.%), indicating effective purification. In contrast, Zn–CES exhibited a single predominant degradation event between 110.29 and 235.29 °C, with a mass loss of 94.98 wt.%, suggesting higher compositional homogeneity and ester purity, consistent with the GC-FID results. For K–CES, multiple degradation stages were observed, although the low residual mass (1.59 wt.%) also confirmed effective purification. Overall, the thermal behaviour of the biodiesel samples was consistent with the catalytic performance and product quality previously discussed.

Figure 11. TGA and DTG curves of biodiesel samples produced using different catalysts.

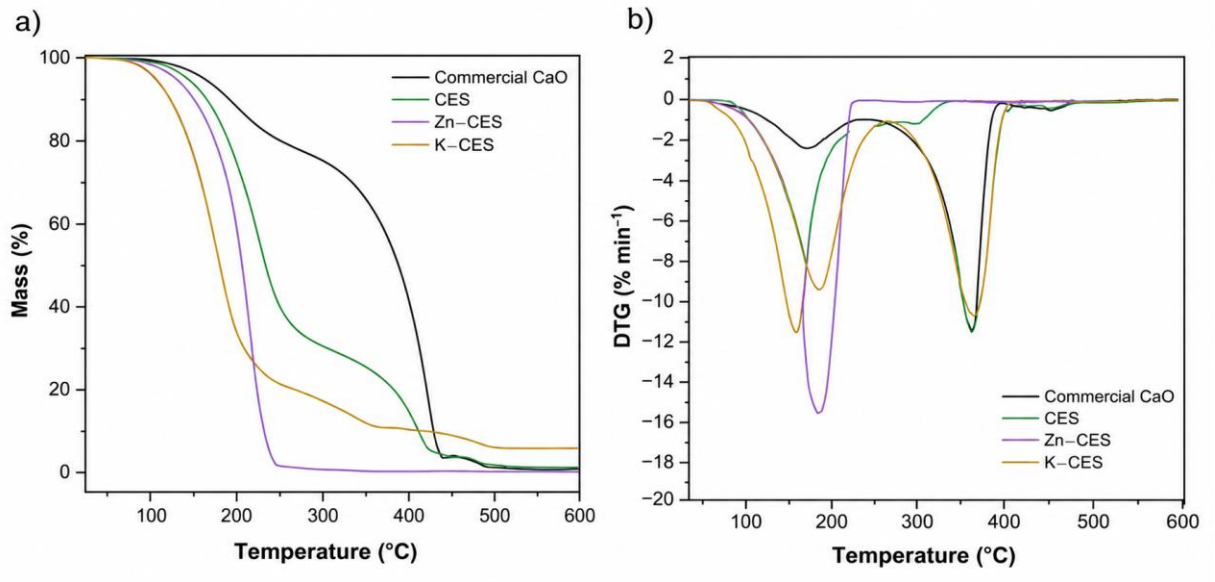


Table 8. Main thermal degradation events identified for biodiesel samples produced using different catalysts.

Catalyst	Event	Degradation range (°C)	Mass loss (wt.%)	Residue (wt.%)
Commercial CaO	I	124.27–234.27	19.28	1.99
	II	279.27–409.27	69.91	—
CES	I	90.78–240.78	21.35	0.50
	II	285.78–410.78	69.35	—
	III	445.78–475.78	1.39	—
Zn–CES	I	110.29–235.29	94.98	1.24
K–CES	I	97.13–262.13	69.69	1.59
	II	317.13–397.13	18.54	—
	III	442.13–482.13	1.24	—

4.4.3 Ester profile by GC-FID

The GC-FID chromatograms of the biodiesel samples are presented in Fig. 12, and the corresponding ester contents are summarised in Table 9. The chromatographic profiles confirmed the formation of fatty acid methyl esters (FAME), characteristic of coconut oil-derived biodiesel, demonstrating the effective conversion of triglycerides during transesterification. Among the catalysts evaluated, Zn–CES exhibited the highest ester content (98.1%), indicating superior selectivity towards methyl ester formation. This behaviour suggests that Zn incorporation modified the catalyst surface, favouring transesterification while suppressing side reactions such as saponification. Although K–CES exhibited lower ester purity than Zn–CES, it still showed a substantial ester content (74.06%) combined with the highest biodiesel yield, reinforcing its superior catalytic activity. Overall, the GC-FID results were consistent with the FTIR, kinetic, and catalytic performance data, confirming the effectiveness of the eggshell-derived catalysts for coconut oil biodiesel production.

Figure 12. GC-FID chromatograms of biodiesel samples produced from coconut oil using commercial CaO (a), CES (b), Zn–CES (c), and K–CES (d) catalysts.

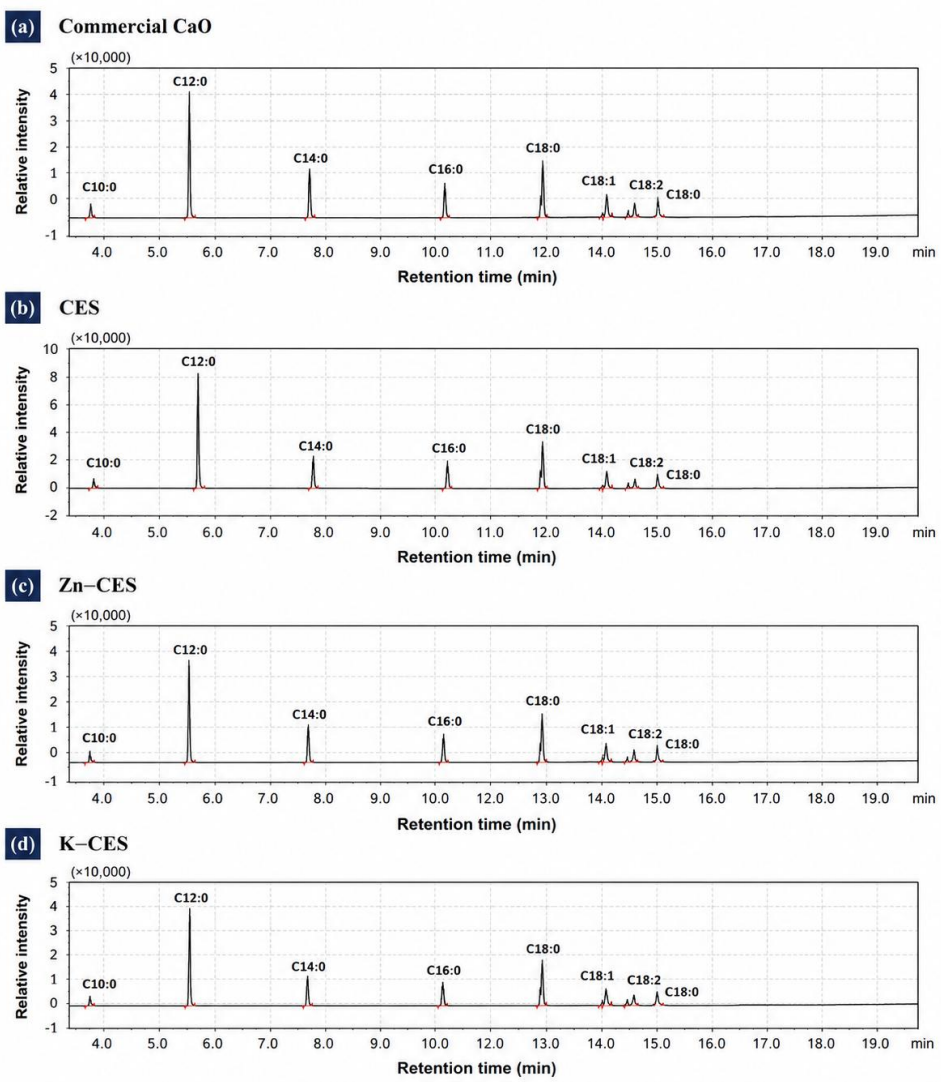


Table 9. Ester content of biodiesel samples obtained using different catalytic systems.

Catalyst	Ester content (wt.%)
Commercial CaO	60.56
CES	63.51
K–CES	74.06
Zn–CES	98.10

4.4.4 Physicochemical properties

The physicochemical properties of the biodiesel samples are presented in Table 10. Kinematic viscosity and density are critical parameters affecting fuel atomisation, combustion efficiency, and engine performance. According to Brazilian specifications (ANP Resolution No. 920), biodiesel viscosity should range between 3.0 and 5.0 $mm^2\ s^{-1}$.

Among the evaluated samples, biodiesel produced using Zn–CES and K–CES exhibited viscosity values within the specification limits, with values of 3.9568 and 3.9769 $mm^2\ s^{-1}$, respectively. In contrast, biodiesel obtained using CES exhibited higher viscosity, suggesting the presence of residual glycerides or incomplete conversion.

All samples showed density values within the regulatory limits, confirming suitable fuel quality. These results are consistent with the GC-FID and FTIR analyses, further confirming the improved product quality obtained using the modified catalysts.

4.5 Proposed catalytic mechanism

Based on the physicochemical characterisation, catalytic performance, kinetic modelling, and biodiesel composition analyses, a reaction mechanism is proposed to elucidate the effect of catalyst modification on coconut oil transesterification. The proposed mechanism highlights how surface basicity, adsorption behaviour, and active site distribution govern both biodiesel yield and ester selectivity, explaining the distinct catalytic responses observed for K–CES and Zn–CES.

4.5.1 Methanol activation on CaO basic sites

The catalytic activity of CaO-based materials is mainly associated with exposed oxygen-containing basic sites at the catalyst surface. During transesterification, these sites promote methanol adsorption and deprotonation, leading to the formation of surface methoxide species, which initiate the nucleophilic attack on triglyceride carbonyl groups and promote the sequential formation of tetrahedral intermediates, fatty acid methyl esters (FAME), and glycerol.

The efficiency of this mechanism strongly depends on the density, accessibility, and physicochemical properties of the active surface sites, which can be significantly modified by chemical treatment, directly influencing catalytic activity, reaction kinetics, and ester selectivity.

4.5.2 Effect of KOH incorporation

Potassium incorporation is proposed to have enhanced the density and accessibility of catalytically active basic environments in the eggshell-derived CaO catalyst, as reflected by the highest biodiesel yield and apparent kinetic constant observed for K–CES. This behaviour can be associated with the formation of potassium-containing phases, particularly K_2O, identified by XRD, which may increase surface basicity and promote methanol activation. As a result, methoxide formation is accelerated, favouring faster triglyceride conversion and higher biodiesel yields. However, highly basic catalytic sites may also promote secondary reactions, particularly saponification involving free fatty acids or residual glycerides, which may explain why K–CES, despite exhibiting the highest catalytic activity, did not achieve the highest ester purity.

4.5.3 Effect of ZnO incorporation

In contrast to K–CES, Zn incorporation appears to promote a more selective catalytic behaviour, as evidenced by the highest ester content obtained for Zn–CES. This suggests that Zn modification influenced not only catalytic performance, but also the reaction pathway. This behaviour may be associated with the formation of possible Ca–O–Zn interfacial environments, which may favour controlled methanol activation while reducing excessive surface basicity. As a result, secondary reactions, particularly saponification, may be suppressed, contributing to higher ester purity and lower by-product formation. In addition, Zn incorporation appears to influence adsorption and catalyst–substrate interactions, promoting more selective conversion of triglycerides into methyl esters. These observations are consistent with the thermal, chromatographic, and kinetic analyses, which confirmed the improved product quality obtained with Zn–CES.

4.5.4 Relationship between activity and selectivity

The results obtained in this study demonstrate a clear relationship between catalytic activity and selectivity in modified eggshell-derived CaO catalysts. K–CES exhibited superior catalytic activity and faster reaction kinetics, which can be associated with enhanced surface basicity and more efficient methanol activation. In contrast, Zn–CES showed lower biodiesel yield but significantly higher ester purity, indicating improved selectivity towards the

transesterification reaction. These findings demonstrate that catalyst modification can be strategically employed to tune the balance between reaction rate and product quality. Highly basic catalytic sites favour rapid triglyceride conversion, whereas more controlled surface environments suppress secondary reactions and improve ester selectivity. Overall, the catalytic behaviour observed in this work highlights the critical role of catalyst composition, surface basicity, and active site distribution in determining transesterification performance, providing valuable insights for the rational design of sustainable heterogeneous catalysts for biodiesel production.

5 Conclusions

Taken together, the results of this study demonstrate that waste-derived eggshell CaO catalysts can be effectively engineered through chemical surface modification to control catalytic activity and selectivity during coconut oil transesterification. Structural, compositional, and thermal analyses confirmed the successful conversion of $CaCO_3$ into catalytically active CaO, as well as the effective incorporation of potassium- and zinc-containing surface species.

The catalytic results revealed a clear activity–selectivity trade-off induced by surface engineering. K–CES exhibited the highest catalytic activity, achieving a biodiesel yield of 86.9% and the highest apparent kinetic constant, consistent with a reaction-controlled mechanism promoted by enhanced surface basicity. In contrast, Zn–CES achieved the highest ester content (98.1%) and showed stronger agreement with adsorption-influenced kinetics, indicating improved product selectivity and suppression of secondary reactions.

Comprehensive biodiesel characterisation by FTIR, GC-FID, TG/DTG, viscosity, and density analyses confirmed the production of high-quality fatty acid methyl esters compliant with fuel quality standards.

Although direct measurements of surface basicity, metal leaching, and catalyst reusability were beyond the scope of the present work, the combined structural, kinetic, chromatographic, and physicochemical analyses provide consistent mechanistic evidence supporting the proposed catalytic behaviour.

Overall, this work demonstrates that chemical modification enables the rational tuning of activity and selectivity in waste-derived CaO catalysts, establishing a practical mechanistic framework for the design of sustainable heterogeneous catalysts within circular biofuel production systems.

List of Abbreviations

ANP	Agência Nacional do Petróleo, Gás Natural e Biocombustíveis (Brazilian National Agency of Petroleum, Natural Gas and Biofuels)
API	Peak area of the internal standard
ATR	Attenuated total reflectance
CES	Calcined eggshell
CPI	Concentration of the internal standard
DTG	Derivative thermogravimetry
EDS	Energy-dispersive X-ray spectroscopy
ES	Eggshell
FAME	Fatty acid methyl esters
FTIR	Fourier-transform infrared spectroscopy
FT-IR	Fourier-transform infrared spectroscopy
GC-FID	Gas chromatography with flame-ionization detection
K–CES	KOH-modified calcined eggshell
KOH	Potassium hydroxide
MeOH	Methanol
SDD	Silicon drift detector
SEM	Scanning electron microscopy
TG	Thermogravimetry; also used for triglyceride in the reaction equations
TGA	Thermogravimetric analysis
XRD	X-ray diffraction
XRF	X-ray fluorescence
Zn–CES	ZnO-modified calcined eggshell
ZnO	Zinc oxide

Declarations

Conflict Of Interest Statement: No potential conflict of interest was reported by the authors.

Funding Information: The authors declare that no funds, grants, or other financial support were received for this research.

References

[1] AZIZ, Saddam et al. Emerging trends and approaches for designing net-zero low-carbon integrated energy networks: A review of current practices. Arabian Journal for Science and Engineering, v. 49, n. 5, p. 6163-6185, 2024. DOI: https://doi.org/10.1007/s13369-023-08336-0

[2] OSHILALU, Adeyemi Zaheed; IBOH, Shalom. Integration of renewable energy technologies into transportation infrastructure to minimize carbon footprint and enhance long-term environmental resilience. Global Journal of Engineering and Technology Advances, v. 24, n. 03, p. 236-251, 2025. DOI: https://doi.org/10.30574/gjeta.2025.24.3.0281

[3] SAEED, Syed; SIRAJ, Tanvir. Global renewable energy infrastructure:: pathways to carbon neutrality and sustainability. Solar energy and sustainable development journal, v. 13, n. 2, p. 183-203, 2024. DOI: https://doi.org/10.51646/jsesd.v13i2.243

[4] NAGAPPAN, M. et al. Alternate fuels for internal combustion engines: Status review on improving performance and reducing emissions with biodiesel, bio-alcohol, bio-oil and plastic oil. Environmental Progress & Sustainable Energy, p. e70485, 2026. DOI: https://doi.org/10.1002/ep.70485

[5] GUDURU, VNSR Ratnakara Rao et al. A comprehensive review on biodiesel performance: advantages, challenges, policies and prospects. International Journal of Oil, Gas and Coal Technology, v. 38, n. 2, p. 240-282, 2025. DOI: https://doi.org/10.1504/IJOGCT.2025.148041

[6] SENUSI, Wardah et al. Biodiesel production and characteristics from waste frying oils: sources, challenges, and circular economic perspective. Environmental Science and Pollution Research, v. 31, n. 23, p. 33239-33258, 2024. DOI: https://doi.org/10.1007/s11356-024-33533-1

[7] SENUSI, Wardah et al. Biodiesel production and characteristics from waste frying oils: sources, challenges, and circular economic perspective. Environmental Science and Pollution Research, v. 31, n. 23, p. 33239-33258, 2024. DOI: https://doi.org/10.1007/s11356-024-33533-1

[8] DAMIAN, Christopher Selvam; DEVARAJAN, Yuvarajan; T, Raja. Nanocatalysts in biodiesel production: advancements, challenges, and sustainable solutions. ChemBioEng Reviews, v. 12, n. 2, p. e202400055, 2025. DOI: https://doi.org/10.1002/cben.202400055

[9] KRISHNAN, M. Gowthama; RAJKUMAR, Sundararajan; DEVASAGAR, T. The sustainable prospect of biodiesel production: transformative technologies, catalysts from bio-wastes, and techno-economic assessment. Materials Today: Proceedings, 2024. DOI: https://doi.org/10.1016/j.matpr.2024.03.005

[10] BORTHAKUR, Partha Protim; BORTHAKUR, Barbie. The role of industrial catalysts in accelerating the renewable energy transition. Chemistry Proceedings, v. 17, n. 1, p. 6, 2025. DOI: https://doi.org/10.3390/chemproc2025017006

[11] BAABUA, Ketshepile et al. Biodiesel synthesis using waste cooking oil via transesterification over heterogeneous inorganic perovskites catalysts: a study of co-solvent effect and surface thermodynamics. Discover Catalysis, v. 3, n. 1, p. 8, 2026. DOI: https://doi.org/10.1007/s44344-026-00037-8

[12] EL MARJI, Lea et al. A Comparative Review of Biomass Conversion to Biodiesel with a Focus on Sunflower Oil: Production Pathways, Sustainability, and Challenges. Processes, v. 14, n. 3, p. 441, 2026. DOI: https://doi.org/10.3390/pr14030441

[13] LARIMI, Afsanehsadat et al. Aspects of reaction engineering for biodiesel production. Catalysts, v. 14, n. 10, p. 701, 2024. DOI: https://doi.org/10.3390/catal14100701

[14] OLIVEIRA, P. A. et al. Ultrasound is a powerful tool for monitoring real-time online transesterification reaction. Fuel, v. 410, p. 137861, 2026. DOI: https://doi.org/10.1016/j.fuel.2025.137861

[15] BHAN, Suraj et al. Innovative catalytic approaches for optimizing biodiesel production: A review of homogeneous, heterogeneous, enzymatic, and nanostructured catalysts. Environmental Progress & Sustainable Energy, v. 44, n. 5, p. e70052, 2025. DOI: https://doi.org/10.1002/ep.70052

[16] ZHENG, Fangyuan; CHO, Haeng Muk. Study on biodiesel production: feedstock evolution, catalyst selection, and influencing factors analysis. Energies, v. 18, n. 10, p. 2533, 2025. DOI: https://doi.org/10.3390/en18102533

[17] RUTAH, Dhishna Fanish; MUDHOO, Ackmez; SURROOP, Dinesh. Effects of process parameters on transesterification of waste cooking oil for biodiesel production: a review. Chemical Papers, p. 1-31, 2026. DOI: https://doi.org/10.1007/s11696-026-04742-4

[18] JAHNAVI, Patibandla et al. Recent Progress in Heterogeneous Catalysis for Sustainable Chemical Processes. J. Chem. Rev, v. 8, n. 2, p. 154-179, 2026. DOI: https://doi.org/10.48309/JCR.2026.535464.1482

[19] LAKHANI, Pratikkumar; BHANDERI, Dhavalkumar; MODI, Chetan K. Support materials impact on green synthesis and sustainable processing via heterogeneous catalysis. Discover Catalysis, v. 1, n. 1, p. 2, 2024. DOI: https://doi.org/10.1007/s44344-024-00002-3

[20] MONDAL, Sujan et al. Sustainable porous heterogeneous catalysts for the conversion of biomass into renewable energy products. ACS Sustainable Resource Management, v. 1, n. 8, p. 1672-1704, 2024. DOI: https://doi.org/10.1021/acssusresmgt.4c00190

[21] LAKHANI, Pratikkumar; SRIFA, Atthapon. Emerging Heterogeneous Catalysis for Valorization of Biomass-Derived Platform Molecules: The Systematic Review Toward Sustainable Biorefinery Applications. Advanced Energy and Sustainability Research, v. 7, n. 2, p. e202500402, 2026. DOI: https://doi.org/10.1002/aesr.202500402

[22] BA TARFI, Abdulrahman S.; BIN NAKQEEB, Mohammed N.; ONAIZI, Sagheer A. Recent advances in carbon dioxide capture using calcium oxide promoted with molten salts: A comprehensive review. Journal of Materials Science, p. 1-44, 2025. DOI: https://doi.org/10.1007/s10853-025-11548-4

[23] SURTIPAL, Sharma et al. Calcium Oxide Nanoparticles as Green Nanocatalysts in Multicomponent Heterocyclic Synthesis: Mechanisms, Metrics, and Future Directions. Catalysts, v. 15, n. 10, p. 970, 2025. DOI: 10.3390/catal15100970

[24] TEO, Chook Kiong et al. Calcium oxide waste-based catalysts for biodiesel production and depollution: a review. Environmental Chemistry Letters, v. 22, n. 4, p. 1741-1758, 2024. DOI: https://doi.org/10.1007/s10311-024-01740-4

[25] ZHANG, Zhuangzhuang et al. Lewis acid-base site-assisted in situ transesterification catalysis to produce biodiesel. Catalysts, v. 14, n. 10, p. 731, 2024. DOI: https://doi.org/10.3390/catal14100731

[26] CHANTHON, Narita et al. Metal loading on CaO/Al2O3 pellet catalyst as a booster for transesterification in biodiesel production. Renewable Energy, v. 218, p. 119336, 2023. DOI: https://doi.org/10.1016/j.renene.2023.119336

[27] TAVIZÓN-POZOS, Jesús Andrés et al. Biodiesel production using K–Sr/CaO and CaO catalysts derived from eggshells by canola oil transesterification. ACS omega, v. 10, n. 7, p. 6827-6838, 2025. DOI: 10.1021/acsomega.4c09118

[28] HART, Abarasi. Circular economy: closing the catalyst loop with metal reclamation from spent catalysts, industrial waste, waste shells and animal bones. Biomass Conversion and Biorefinery, v. 13, n. 13, p. 11483-11498, 2023. DOI: https://doi.org/10.1007/s13399-021-01942-8

[29] DONG, Zhaolin et al. Progress and challenges in the process of using solid waste as a catalyst for biodiesel synthesis. Molecules, v. 30, n. 15, p. 3243, 2025. DOI: https://doi.org/10.3390/molecules30153243

[27] RUTSA, Vilabeilie; YIMCHUNGER, Akhiu K.; SINGH, Ambrish. Introduction and fundamentals of waste-derived catalysts. In: Waste Derived Catalysts. Elsevier, 2026. p. 3-25. DOI: https://doi.org/10.1016/B978-0-443-32958-6.00001-7

[28] GUPTA, Deepshikha et al. Green catalyst solutions from waste for sustainable treatment processes. In: Waste Derived Catalysts. Elsevier, 2026. p. 277-309. DOI: https://doi.org/10.1016/B978-0-443-32958-6.00014-5

[29] MACHELI, Lebohang et al. Enhancing waste eggshell-derived CaO catalysts for biodiesel production through synergistic oxide modification: a comprehensive catalytic and kinetic study. RSC advances, v. 16, n. 7, p. 5990-6001, 2026. DOI: https://doi.org/10.1039/D5RA06382E

[30] FRANCIS, Adel A. Ecologic and economic motives for transforming calcium-based food wastes into sustainable value-added products: A review. Environmental Science and Pollution Research, v. 32, n. 2, p. 428-451, 2025. DOI: https://doi.org/10.1007/s11356-024-35649-w

[31] TEO, Chook Kiong et al. Calcium oxide waste-based catalysts for biodiesel production and depollution: a review. Environmental Chemistry Letters, v. 22, n. 4, p. 1741-1758, 2024. DOI: https://doi.org/10.1007/s10311-024-01740-4

[32] WANG, Jingxiao et al. Research Progress and Key Technical Barriers in CaO/Ca (OH) 2 Based Energy Storage: A Systematic Review. Clean Energy and Sustainability, v. 3, n. 2, p. 10005, 2025. DOI: https://doi.org/10.70322/ces.2025.10005

[33] GARCÍA, Yusbeli C.; GRASA, Gemma; MARTÍNEZ, Isabel. Sorption-Enhanced Methanation Using CaO-and Ni-Based Catalysts as Functional Materials. Energy & Fuels, v. 39, n. 9, p. 4304-4314, 2025. DOI: https://doi.org/10.1021/acs.energyfuels.4c04828

[34] GARCÍA, Yusbeli C.; MARTÍNEZ, Isabel; GRASA, Gemma. Determination of the hydration and carbonation kinetics of CaO for low-temperature applications. Chemical Engineering Science, v. 295, p. 120146, 2024. DOI: https://doi.org/10.1016/j.ces.2024.120146

[35] CHEN, Xuetao et al. Enhanced cyclic stability of CaO-based composite metal oxides for CO2 capture at high temperatures. Chemical Engineering Journal, p. 172001, 2025. DOI: https://doi.org/10.1016/j.cej.2025.172001

[36] SHOKROLLAHI YANCHESHMEH, Marziehossadat; ILIUTA, Maria C. Embedding Ni in Ni–Al mixed-metal alkoxide for the synthesis of efficient coking resistant Ni–CaO-based catalyst-sorbent bifunctional materials for sorption-enhanced steam reforming of glycerol. ACS Sustainable Chemistry & Engineering, v. 8, n. 45, p. 16746-16756, 2020. DOI: https://doi.org/10.1021/acssuschemeng.0c03859

[37] VENKATESH, Yatish Kalanakoppal et al. Developments in Titanium-Based Alkali and Alkaline Earth Metal Oxide Catalysts for Sustainable Biodiesel Production: A Review. The Chemical Record, v. 23, n. 12, p. e202300277, 2023. DOI: https://doi.org/10.1002/tcr.202300277

[38] BA TARFI, Abdulrahman S.; BIN NAKQEEB, Mohammed N.; ONAIZI, Sagheer A. Recent advances in carbon dioxide capture using calcium oxide promoted with molten salts: A comprehensive review. Journal of Materials Science, p. 1-44, 2025. DOI: https://doi.org/10.1007/s10853-025-11548-4

[39] LI, Xiangyang et al. Catalytic properties and structural optimization of solid transesterification catalysts to enhance the efficiency of biodiesel synthesis. Catalysts, v. 15, n. 3, p. 239, 2025. DOI: https://doi.org/10.3390/catal15030239

[40] ZHANG, Shunpan et al. Sodium silicates modified calcium oxide as a high-performance solid base catalyst for biodiesel production. Catalysts, v. 13, n. 4, p. 775, 2023. DOI: https://doi.org/10.3390/catal13040775

[41] OZOR, Paul Amaechi; AIGBODION, Victor Sunday; SUKDEO, Nita Inderlal. Modified calcium oxide nanoparticles derived from oyster shells for biodiesel production from waste cooking oil. Fuel Communications, v. 14, p. 100085, 2023. DOI: https://doi.org/10.1016/j.jfueco.2023.100085

[42] OZOR, Paul Amaechi; AIGBODION, Victor Sunday; SUKDEO, Nita Inderlal. Modified calcium oxide nanoparticles derived from oyster shells for biodiesel production from waste cooking oil. Fuel Communications, v. 14, p. 100085, 2023. DOI: https://doi.org/10.1016/j.fuel.2022.124387

[43] ELOUAHED, Salima Kouider et al. Optimization of the activity of Mo7-Zn3/CaO catalyst in the transesterification of waste cooking oil into sustainable biodiesel via response surface methodology. Energy Conversion and Management, v. 303, p. 118185, 2024. DOI: https://doi.org/10.1016/j.enconman.2024.118185

[44] CAO, Yueqiang et al. Configuration Matching Strategy to Control Selectivity in Heterogeneous Catalysis. Accounts of Chemical Research, v. 59, n. 1, p. 126-137, 2025. DOI: https://doi.org/10.1021/acs.accounts.5c00671

[45] WANG, Haiyan et al. Thermochemical conversion of biomass to fuels and chemicals: A review of catalysts, catalyst stability, and reaction mechanisms. Catalysis Reviews, v. 67, n. 1, p. 57-129, 2025. DOI: https://doi.org/10.1080/01614940.2023.2275093

[46] YE, Runping et al. Design of catalysts for selective CO2 hydrogenation. Nature Synthesis , v. 4, n. 3, p. 288-302, 2025. DOI: https://doi.org/10.1038/s44160-025-00747-1

[47] FANG, Zicheng et al. Noble metal catalysts for methanol steam reforming: advances and future directions for hydrogen production. Journal of Materials Chemistry A, v. 14, n. 18, p. 10505-10523, 2026. DOI: https://doi.org/10.1039/D5TA08853D

[48] Potorochenko, AN.; Rodygin KS. Toward CO2-neutral biodiesel production: industrial challenges and advances in CaO-based catalysts. Carbon Footprints 2026, 5, 14. DOI: https://dx.doi.org/10.20517/cf.2025.101

[49] DIAS, Ana Paula Soares; RAMOS, Marta. On the storage stability of CaO biodiesel catalyst. Hydration and carbonation poisoning. Journal of Environmental Chemical Engineering, v. 9, n. 1, p. 104917, 2021. DOI: https://doi.org/10.1016/j.jece.2020.104917

[50] MACHELI, Lebohang; MALEFANE, Mope Edwin; JEWELL, Linda L. Waste-derived calcium oxide catalysts in biodiesel production: Exploring various waste sources, deactivation challenges, and improvement strategies. Bioresource Technology Reports, v. 29, p. 102021, 2025. DOI: https://doi.org/10.1016/j.biteb.2025.102021

[51] TABANAG, Ian Dominic F. et al. Esterification of Coconut Fatty Acid Distillate (COFAD) Using Hydrochloric Acid as Homogeneous Acid Catalyst: A Kinetic and Thermodynamic Analysis. Engineering Chemistry, v. 12, p. 49-71, 2025. DOI: https://doi.org/10.4028/p-6kVCnm

[52] NIKOLIĆ, Boban D. et al. Biodiesel and feedstocks-possibilities and characteristics: A review. Thermal Science, n. 00, p. 58-58, 2025. DOI: https://doi.org/10.2298/TSCI250205058N

[53] PERUMAL, Govindhan et al. A systematic review on the production of biodiesel using various feedstocks and effective catalysts. Petroleum Science and Technology, v. 43, n. 15, p. 1910-1926, 2025. DOI: https://doi.org/10.1080/10916466.2024.2366464

[54] AHMAD, Aisyah Fathiah et al. Catalytic transesterification of coconut oil in biodiesel production: a review. Catalysis Surveys from Asia, v. 26, n. 3, p. 129-143, 2022. DOI: https://doi.org/10.1007/s10563-022-09358-8

[55] KANNAN, Rajesh et al. Optimization and synthesis process of biodiesel production from coconut oil using central composite rotatable design of response surface methodology. Proceedings of the Institution of Mechanical Engineers, Part E: Journal of Process Mechanical Engineering, v. 239, n. 6, p. 3314-3324, 2025. DOI: https://doi.org/10.1177/09544089241230251

[56] YAO, Xingjun et al. Kinetic Aspects of Esterification and Transesterification in Microstructured Reactors. Molecules, v. 29, n. 15, p. 3651, 2024. DOI: https://doi.org/10.3390/molecules29153651

[57] OH, Myungwon et al. Importance of pore size and Lewis acidity of Pt/Al2O3 for mitigating mass transfer limitation and catalyst fouling in triglyceride deoxygenation. Chemical Engineering Journal, v. 439, p. 135530, 2022. DOI: https://doi.org/10.1016/j.cej.2022.135530

[58] RABAH, Muhammad et al. Review on Carbonaceous Catalysts for Transesterification of Feedstock Toward Biodiesel Production: Advances, Challenges, and AI Perspectives. Energy & Fuels, v. 40, n. 8, p. 3978-4017, 2026. DOI: https://doi.org/10.1021/acs.energyfuels.5c04985

[59] GUPTA, Anilkumar R.; RATHOD, Virendra K. Waste cooking oil and waste chicken eggshells derived solid base catalyst for the biodiesel production: Optimization and kinetics. Waste management, v. 79, p. 169-178, 2018. DOI: https://doi.org/10.1016/j.wasman.2018.07.022

[60] YINGYING, Liu et al. Biodiesel production from crude Jatropha curcas L. oil with trace acid catalyst. Chinese Journal of Chemical Engineering, v. 20, n. 4, p. 740-746, 2012. DOI: https://doi.org/10.1016/S1004-9541(11)60243-7

[61] FEYZI, Mostafa; KHAJAVI, Gelareh. Kinetics study of biodiesel synthesis from sunflower oil using Ba-Sr/ZSM-5 nanocatalyst. 2016.

[62] VOGT, Charlotte; WECKHUYSEN, Bert M. O conceito de sítio ativo em catálise heterogênea. Nature Reviews Chemistry , v. 6, n. 2, p. 89-111, 2022. DOI: https://doi.org/10.1038/s41570-021-00340-y

[63] ZHANG, Hao et al. Dynamic transformation of active sites in energy and environmental catalysis. Energy & Environmental Science, v. 17, n. 18, p. 6435-6481, 2024. DOI: https://doi.org/10.1039/D4EE02365J

[64] LI, Xiangyang et al. Catalytic properties and structural optimization of solid transesterification catalysts to enhance the efficiency of biodiesel synthesis. Catalysts, v. 15, n. 3, p. 239, 2025. DOI: https://doi.org/10.3390/catal15030239

[65] GHAFFARINEJAD, Tara; KARIMZADEH, Ramin. Green biodiesel production through enhanced adsorption using bifunctional ethoxy amine modified silica catalysts. Scientific Reports, 2026. DOI: https://doi.org/10.1038/s41598-026-41400-x

[66] GAURAV, Kumar; KUMARI, Soni; DUTTA, Joydeep. Utilization of waste chicken eggshell as heterogeneous CaO nanoparticle for biodiesel production. Journal of Biochemical Technology, v. 12, n. 1-2021, p. 49-57, 2021. DOI: https://doi.org/10.51847/eqTib7hM7Z

[67] MMUSI, Keene Carlvin; ODISITSE, Sebusi; NAREETSILE, Florence. Comparison of CaO-NPs and Chicken Eggshell-Derived CaO in the Production of Biodiesel from Schinziophyton rautanenii (Mongongo) Nut Oil. Journal of Chemistry, v. 2021, n. 1, p. 6663722, 2021. DOI: https://doi.org/10.1155/2021/6663722

[68] HEMMAMI, Hadia et al. Green synthesis of CaO nanoparticles from chicken eggshells: antibacterial, antifungal, and heavy metal ($Pb2^{+}$, $Cr2^{+}$, $Cd2^{+}$ and $Hg2^{+}$) adsorption properties. Frontiers in Environmental Science, v. 12, p. 1450485, 2024. DOI: https://doi.org/10.3389/fenvs.2024.1450485

[69] SULAIMAN, Nur Fatin et al. Transition metal oxide (NiO, CuO, ZnO)-doped calcium oxide catalysts derived from eggshells for the transesterification of refined waste cooking oil. RSC advances, v. 11, n. 35, p. 21781-21795, 2021. DOI: https://doi.org/10.1039/D1RA02076E

[70] WICAKSONO, Dino; KUSUMANINGTYAS, Ratna Dewi. Synthesis of ZnO/CaO catalyst from eggshell waste for biodiesel production. Jurnal Bahan Alam Terbarukan, v. 8, n. 1, p. 65-71, 2019. DOI: https://doi.org/10.15294/jbat.v8i1.20185

[71] HA, Jeyoung; LEE, Sungho; LI, Oi Lun. High-efficiency biodiesel production using ZnO-modified starfish-based catalysts. Catalysts, v. 15, n. 4, p. 372, 2025. DOI: https://doi.org/10.3390/catal15040372

[72] LANZÓN, Marcos et al. Use of eggshell waste: A green and effective method for the synthesis of pure calcium hydroxide suspensions. Construction and Building Materials, v. 377, p. 131106, 2023. DOI: https://doi.org/10.1016/j.conbuildmat.2023.131106

[73] KALAYCI, Taner et al. Characterization and potential usage of selected eggshell species. Scientific Reports, v. 15, n. 1, p. 6241, 2025. DOI: https://doi.org/10.1038/s41598-025-87786-y

[74] AHMED, Naziha Sultan et al. Calcium carbonate nanoparticles of quail's egg shells: Synthesis and characterizations. Journal of the Mechanical Behavior of Materials, v. 31, n. 1, p. 1-7, 2022. DOI: https://doi.org/10.1515/jmbm-2022-0001

[75] ZIA, Jannatun; SHRINGI, Amit Kumar; RIAZ, Ufana. Calcium oxide nanoparticles from eggshell waste: A green nanotechnological strategy for microwave-assisted environmental clean up. Cleaner Chemical Engineering, v. 11, p. 100182, 2025. DOI: https://doi.org/10.1016/j.clce.2025.100182

[76] MAZ ISA, A. A. et al. Physicochemical Characterization of CaO Derived from Pearl Oyster Shells (Pinctada maxima) via Thermal Processing for Potential Biomedical Applications. In: Journal of Physics: Conference Series. IOP Publishing, 2025. p. 012027. DOI: 10.1088/1742-6596/3139/1/012027

[77] USMAN, Abdulrahman S. et al. Calcium Oxide Derived from Okpella Limestone as a Heterogeneous Catalyst for Biodiesel Production: Synthesis, Characterisation and Stability Assessment. FUDMA Journal of Engineering and Technology, v. 1, n. 2, p. 863-875, 2025. DOI: https://doi.org/10.33003/bne6wb50

[78] THABET, Ihab Adnan; AL-JAWAD, Selma MH; TAHA, Ali A. Evaluating Calcium Overload by Pure and Ag-Doped CaO Nanoparticles for Cancer Therapy. Plasmonics, v. 21, n. 2, p. 1615-1635, 2026. DOI: https://doi.org/10.1007/s11468-025-03318-4

[79] KOUIDER ELOUAHED, Salima et al. Efficient biodiesel production from soybean oil using calcium oxide supported bimetallic molybdenum-zinc catalysts. International Journal of Green Energy, v. 22, n. 16, p. 3670-3686, 2025. DOI: https://doi.org/10.1080/15435075.2025.2528392

[80] SILVESTER, C. Deepan et al. Plant Extract-Mediated Valorization of Eggshell Waste into a Multifunctional CuO− ZnO/HAP Biocomposite for Sustainable Biological and Photocatalytic Applications. ACS Sustainable Resource Management, 2026. DOI: https://doi.org/10.1021/acssusresmgt.6c00069

[81] ARREDONDO-TAMAYO, Benjamín et al. Hierarchical Roughness-Engineered Superhydrophobic Coatings: A Sustainable Approach Using Eggshell Waste and ZnO Nanoparticles. ChemistrySelect, v. 11, n. 1, p. e05456, 2026. DOI: https://doi.org/10.1002/slct.202505456

[82] TAVIZÓN-POZOS, Jesús Andrés et al. Biodiesel production using K–Sr/CaO and CaO catalysts derived from eggshells by canola oil transesterification. ACS omega, v. 10, n. 7, p. 6827-6838, 2025. DOI: https://doi.org/10.1021/acsomega.4c09118

[83] OLVERA-UREÑA, E. et al. Dispersion of Sr and K species supported on CaO eggshell-based catalysts for biodiesel production. Topics in Catalysis, v. 68, n. 14, p. 1777-1790, 2025. DOI: https://doi.org/10.1007/s11244-025-02050-x

[84] ERAIAH, B. et al. Optical and physical properties of eggshell-derived CaO-doped potassium titanium phosphate bioactive glasses. Applied Physics A, v. 131, n. 10, p. 1-15, 2025. DOI: https://doi.org/10.1007/s00339-025-08914-z

[85] ETIM, Anietie O.; MUSONGE, P. Process analysis and optimization of biocompatible diesel production from blended vegetable oils using KOH-impregnated eggshells derived CaO catalyst. Green Technologies and Sustainability, p. 100262, 2025. DOI: https://doi.org/10.1016/j.grets.2025.100262

[86] AKTER, Taslima et al. Effect of reaction parameters on CO2 absorption from biogas using CaO sorbent prepared from waste chicken eggshell. ACS omega, v. 8, n. 45, p. 43000-43007, 2023. DOI: https://doi.org/10.1021/acsomega.3c06226

[87] MOHADI, Risfidian et al. Calcium oxide catalyst based on quail eggshell for biodiesel synthesis from waste palm oil. The Journal of Pure and Applied Chemistry Research, v. 7, n. 2, p. 130, 2018. DOI: 10.21776/ub.jpacr.2018.007.02.390

[88] KIRUBAKARAN, M.; SELVAN, V. Arul Mozhi. Experimental investigation on the effects of micro eggshell and nano-eggshell catalysts on biodiesel optimization from waste chicken fat. Bioresource Technology Reports, v. 14, p. 100658, 2021. DOI: https://doi.org/10.1016/j.biteb.2021.100658

[89] MOHAMMED, Adem Siraj; ANCHA, Venkata Ramaya; ATNAW, Samson Mekbib. Optimization of biodiesel production from Croton Macrostachyus seed oil with calcium oxide (CaO) catalyst and Characterization: Potential assessment of seed and kernel. Energy Conversion and Management: X, v. 24, p. 100791, 2024. DOI: https://doi.org/10.1016/j.ecmx.2024.100791

[90] SAIF, Asima et al. Comparison of catalytic applications of CaO-Ag bimetallic nanoparticles and its composite: CaO-Ag/Na-alg/PANI. Journal of Inorganic and Organometallic Polymers and Materials, v. 35, n. 5, p. 3344-3365, 2025. DOI: https://doi.org/10.1007/s10904-024-03460-2

[91] ARENAS-QUEVEDO, M. G. et al. ZnO–doped CaO binary core–shell catalysts for biodiesel production via Mexican palm oil transesterification. Inorganics, v. 12, n. 2, p. 51, 2024. DOI: https://doi.org/10.3390/inorganics12020051

[92] HASAN, Muhammad Rubaiat et al. + exploring the effects of different parameters on the incorporation of K ions in eggshell derived CaO reveals highly variable catalytic efficiency for biodiesel conversion. South African Journal of Chemical Engineering, v. 47, n. 1, p. 67-74, 2024. Available at: https://hdl.handle.net/10520/ejc-chemeng-v47-n1-a8

[93] KUSMIYATI, Kusmiyati et al. Biodiesel production from reutealis trisperma oil using KOH impregnated eggshell as a heterogeneous catalyst. Energies, v. 12, n. 19, p. 3714, 2019. DOI: https://doi.org/10.3390/en12193714

[94] SULAIMAN, Nur Fatin et al. Enhanced transesterification reaction using chromium-doped calcium oxide-based catalyst supported on alumina and its specification of biodiesel. Energy Conversion and Management, v. 293, p. 117556, 2023. DOI: https://doi.org/10.1016/j.enconman.2023.117556

[95] DAI, Gaofeng et al. Calcination and desulfurization characteristics of calcium carbonate in pressurized oxy-combustion. Energy, v. 261, p. 125150, 2022. DOI: https://doi.org/10.1016/j.energy.2022.125150

[96] MA, Weiping et al. An innovative approach to prepare calcium oxide from calcium carbide slag based on sequential mineral transformation. ACS Sustainable Resource Management, v. 1, n. 6, p. 1279-1290, 2024. DOI: https://doi.org/10.1021/acssusresmgt.4c00164

[97] GENG, Rui et al. Structure evolution of Zn species on fresh, deactivated, and regenerated Zn/ZSM-5 catalysts in ethylene aromatization. ACS Catalysis, v. 12, n. 23, p. 14735-14747, 2022. DOI: https://doi.org/10.1021/acscatal.2c04074

Figure titles and legends

Figure 1. Crystal structure of calcium oxide and surface basic sites.
Schematic representation of the ionic crystal structure of calcium oxide (CaO), showing the spatial arrangement of Ca^{2+} and O^{2-} ions and illustrating the origin of surface basic sites associated with methanol activation during transesterification.

Figure 2. Scanning electron micrographs of eggshell-derived catalysts.
SEM micrographs of (a) raw eggshell (ES), (b) calcined eggshell (CES), (c) ZnO-modified calcined eggshell (Zn–CES), and (d) KOH-modified calcined eggshell (K–CES), showing the morphological changes associated with calcination and chemical modification.

Figure 3. X-ray diffraction patterns of eggshell-derived catalysts.
XRD patterns of (a) ES, (b) CES, (c) Zn–CES, and (d) K–CES. The patterns show the crystalline phases identified in the raw eggshell precursor and after calcination and chemical modification.

Figure 4. FTIR spectra of eggshell-derived catalysts.
FTIR spectra of (a) ES, (b) CES, (c) Zn–CES, and (d) K–CES, showing the characteristic absorption bands associated with carbonate, hydroxyl, and other surface-related groups.

Figure 5. EDS spectra of eggshell-derived catalysts.
EDS spectra of (a) ES, (b) CES, (c) Zn–CES, and (d) K–CES, illustrating the elemental signals detected in the raw, calcined, and chemically modified samples.

Figure 6. Thermogravimetric and derivative thermogravimetric profiles of catalyst samples.
TG and DTG curves of (a) ES, (b) CES, (c) Zn–CES, and (d) K–CES, showing the mass-loss behaviour and thermal decomposition features of the catalyst precursors and modified materials.

Figure 7. Effect of reaction time on biodiesel yield.
Biodiesel yield as a function of reaction time during coconut oil transesterification using commercial CaO, CES, Zn–CES, and K–CES catalysts. The figure compares catalytic performance under the reaction conditions described in the Materials and Methods section.

Figure 8. Pseudo-first-order kinetic model for coconut oil transesterification.
Linearized pseudo-first-order kinetic plots for coconut oil transesterification using commercial CaO, CES, Zn–CES, and K–CES catalysts. The plots are used to compare the apparent kinetic behaviour of the catalytic systems.

Figure 9. Pseudo-second-order kinetic model for coconut oil transesterification.
Linearized pseudo-second-order kinetic plots for coconut oil transesterification using commercial CaO, CES, Zn–CES, and K–CES catalysts. The plots are used to evaluate and compare the fit of the pseudo-second-order model to the experimental data.

Figure 10. FTIR spectra of biodiesel products.
FTIR spectra of biodiesel samples produced from coconut oil using commercial CaO, CES, Zn–CES, and K–CES catalysts, showing absorption bands associated with the functional groups present in the products.

Figure 11. Thermogravimetric profiles of biodiesel samples.
TGA and DTG curves of biodiesel samples obtained using the different catalytic systems, showing their thermal decomposition behaviour and mass-loss profiles.

Figure 12. GC-FID chromatograms of biodiesel samples.
GC-FID chromatograms of biodiesel produced from coconut oil using (a) commercial CaO, (b) CES, (c) Zn–CES, and (d) K–CES catalysts, illustrating the chromatographic profiles used to assess the fatty acid methyl ester content of the products.